

## RESEARCH ARTICLE

# The H3K4me3/2 histone demethylase RBR-2 controls axon guidance by repressing the actin-remodeling gene *wsp-1*

Luca Mariani<sup>1,2</sup>, Yvonne C. Lussi<sup>1,2</sup>, Julien Vandamme<sup>1,2,\*</sup>, Alba Riveiro<sup>1,2</sup> and Anna Elisabetta Salcini<sup>1,2,†</sup>

**ABSTRACT**

The dynamic regulation of histone modifications is important for modulating transcriptional programs during development. Aberrant H3K4 methylation is associated with neurological disorders, but how the levels and the recognition of this modification affect specific neuronal processes is unclear. Here, we show that RBR-2, the sole homolog of the KDM5 family of H3K4me3/2 demethylases in *Caenorhabditis elegans*, ensures correct axon guidance by controlling the expression of the actin regulator *wsp-1*. Loss of *rbr-2* results in increased levels of H3K4me3 at the transcriptional start site of *wsp-1*, with concomitant higher *wsp-1* expression responsible for defective axon guidance. In agreement, overexpression of WSP-1 mimics *rbr-2* loss, and its depletion restores normal axon guidance in *rbr-2* mutants. NURF-1, an H3K4me3-binding protein and member of the chromatin-remodeling complex NURF, is required for promoting aberrant *wsp-1* transcription in *rbr-2* mutants and its ablation restores wild-type expression of *wsp-1* and axon guidance. Thus, our results establish a precise role for epigenetic regulation in neuronal development by demonstrating a functional link between RBR-2 activity, H3K4me3 levels, the NURF complex and the expression of WSP-1.

**KEY WORDS:** Epigenetics, H3K4 methylation, Histone demethylase, Neuronal development, Axon guidance, *C. elegans*

**INTRODUCTION**

Chromatin organization regulates gene expression by changing DNA accessibility and is thought to have a key role in developmental processes (Eissenberg and Shilatifard, 2010; Greer and Shi, 2012). Post-translational modifications on the N-terminal tails of histone proteins are one of the elements that can influence chromatin structure. To date, several chromatin factors with the ability to catalyze the addition ('writers') or removal ('erasers') of these modifications have been identified (Zhang and Pradhan, 2014). Modified histones can modulate the strength of DNA/histone interactions as well as recruit ATP-dependent chromatin remodelers and other factors with the ability to decode the modifications ('readers') (Baker et al., 2008). Methylation of lysine 4 on histone 3 (H3K4) is one of the most studied modifications, with its trimethylated form (H3K4me3) enriched at transcriptional start sites (TSSs) of actively transcribed genes (Barski et al., 2007). In mammals, members of the lysine methyltransferase 2 family

(KMT2) catalyze di- and tri-methylation of H3K4 (Eissenberg and Shilatifard, 2010), whereas its demethylation is executed by the four members of the lysine demethylase 5 family (KDM5) (Benevolenskaya, 2007; Pedersen and Helin, 2010; Kooistra and Helin, 2012). The biological consequences of changes in H3K4 methylation are mediated, at least in part, by molecules that recognize methylated forms of H3K4, including the plant homeodomain (PHD) zinc-finger proteins (Baker et al., 2008). The relevance of chromatin organization in many aspects of cell biology is testified by the identification of several chromatin factors that are mutated in cancer (Helin and Dhanak, 2013; Suzuki et al., 2013). Recently, next-generation sequencing approaches have uncovered mutations in genes that encode multiple chromatin regulators in neurodevelopmental and psychiatric disorders, including intellectual disability syndromes, schizophrenia and autism spectrum disorders (for reviews, see Berdasco and Esteller, 2013; Ronan et al., 2013). Interestingly, among the mutated genes, members of the KMT2 (KMT2A/C/D) and KDM5 (KDM5A/B/C) families were identified (Shen et al., 2014; Vallianatos and Iwase, 2015), strongly suggesting that the regulation of H3K4 methylation is important to achieve correct neuronal development and functionality.

Although the catalytic properties of the KDM5 proteins are well established, relatively little is known about their biological functions. Knockout mice have been generated for some of the KDM5 family members and their characterization supports a role for this class of demethylases in neuronal development (Klose et al., 2007; Schmitz et al., 2011; Albert et al., 2013). However, the complexity of the murine nervous system and the early lethality associated with loss of some KDM5 members (Cox et al., 2010; Catchpole et al., 2011; Albert et al., 2013) have challenged the identification of their specific neuronal functions and relevant downstream targets. Thus, the study of the KDM5 family in a biologically relevant but smaller and more tractable model nervous system could provide information regarding the roles of these proteins in different aspects of neuronal development. The KDM5 family is evolutionarily conserved and is represented uniquely by the RBR-2 protein in *Caenorhabditis elegans*. Previous analyses have shown that RBR-2 is a regulator of vulva formation (Christensen et al., 2007) and aging (Greer et al., 2010, 2011), but no data are available regarding its potential function in neuronal development.

The *C. elegans* nervous system is the most complex tissue of the animal both in terms of numbers and diversity of cells. It consists of 302 cells, for which the lineage, morphology, migration patterns and axonal routing have been described (Sulston et al., 1983; White et al., 1986). A large number of evolutionarily conserved secreted molecules, such as Slits, Netrins, Semaphorins and Ephrins, as well as extracellular matrix components, are known to orchestrate neuronal cell migration and axon guidance (reviewed by Hatten, 2002; Hobert and Bülow, 2003; Killeen and Sybingco, 2008).

<sup>1</sup>BioTech Research & Innovation Centre (BRIC), University of Copenhagen, 2200 Copenhagen, Denmark. <sup>2</sup>Centre for Epigenetics, University of Copenhagen, 2200 Copenhagen, Denmark.

\*Present address: Section for Immunology and Vaccinology, National Veterinary Institute, Technical University of Denmark, Denmark.

†Author for correspondence (lis.salcini@bric.ku.dk)

Received 16 November 2015; Accepted 16 January 2016

Similar to mammals, this complex signaling network ultimately regulates the dynamics of actin-based structures controlling neuronal cell migration and axon growth and guidance. Indeed, evolutionarily conserved molecules regulating actin dynamics, such as WSP-1/WASP (WAS), UNC-34/Ena/VASP and WVE-1/WAVE (WASF1), have been shown to contribute to correct axon guidance by integrating multiple signaling pathways (Luo, 2002; Koleske, 2003; Norris et al., 2009; Dent et al., 2011; Mohamed et al., 2012; Chia et al., 2014; Gomez and Letourneau, 2014). The WASP and WAVE protein families, which ensure maximal actin nucleation through the activation of the Arp2/3 complex (Takenawa and Suetsugu, 2007; Pollitt and Insall, 2009), act in response to Netrin and Semaphorins (Zallen et al., 2002; Shekarabi et al., 2005). Similarly, the Ena/VASP proteins, regulating actin dynamics through their anti-capping activity, are downstream targets of the Netrin and Slit pathways (Bashaw et al., 2000; Yu et al., 2002; Gitai et al., 2003; Lebrand et al., 2004; Forsthoefel et al., 2005; Chang et al., 2006).

Here, we describe the role of RBR-2 in neuronal development and the mechanism through which RBR-2 ensures correct neuronal architecture. We show that the H3K4me3 demethylase activity of RBR-2 plays a key function in regulating axon guidance by controlling the transcription of the actin-remodeling gene *wsp-1*. In the *rbr-2* mutant, increased levels of H3K4me3 at the *wsp-1* promoter lead to its overexpression and consequent axon guidance defects. Moreover, we provide evidence that the NURF complex is required for the upregulation of *wsp-1* in the *rbr-2* mutant and therefore for translating the aberrant H3K4me3 signal into developmental failures.

## RESULTS

### RBR-2 is required for correct axon guidance

To identify the potential role of RBR-2 in neuronal development, we used the *rbr-2(tm3141)* mutant allele, which carries an out-of-frame deletion eliminating the catalytic JmjC domain and other conserved domains (Fig. 1A). Notably, the expression of the *rbr-2* locus is markedly reduced (Fig. 1B), suggesting that this allele is probably a strong loss-of-function mutant. *rbr-2(tm3141)* was crossed with transgenic animals carrying GFP reporters specifically expressed in interneurons (PVPs, PVQs, AVKs) and motoneurons (HSNs, DA/DB, DVB, D-type), which allow the identification of neuronal cell bodies and their processes. We also analyzed amphid and phasmid neurons, sensory neurons in direct contact with the environment, by using a diffusible dye (Table 1). The number of analyzed neurons in the *rbr-2(tm3141)* mutant was unaffected, suggesting that RBR-2 is not likely to be involved in the early steps of their neuronal development, e.g. cell fate commitment. By contrast, loss of *rbr-2* led to the aberrant cross-over of axons projected by specific pairs of neurons, namely PVPs, PVQs and HSNs (Fig. 1C), which are positioned in a bilaterally symmetric manner at the right and left sides of the animal. The PVQ and PVP neurons, which fully develop during embryogenesis, are located at the posterior of the animals and project their axons anteriorly to the nerve ring. In wild-type animals, their projections invariably run along the ventral nerve cord (VNC) in two distinct bundles separated by the midline (Boulin et al., 2006). In *rbr-2(tm3141)* mutants, the PVQ and PVP axons failed to maintain the correct trajectory and aberrantly crossed over the midline (Fig. 1C). The HSNs, a pair of motoneurons born during embryogenesis but extending their axon during early larval stages, showed similar axon guidance defects (Fig. 1C). Occasionally the cellular bodies of the HSNs showed also an abnormal positioning in *rbr-2(tm3141)* animals (Table 1; Fig. S1A).

Axon guidance defects were also identified in another *rbr-2* mutant allele (*tm1231*) (Fig. S1B), indicating that *rbr-2* is required for correct axon guidance.

### RBR-2 acts during embryogenesis in the nervous system to ensure correct axon guidance

To study the functional role of RBR-2 in axon guidance, we focused on the PVQ neurons, which fully develop during embryogenesis and are easily visualized by using the *oyIs14* transgene. As several molecules have been shown to play a role in maintaining rather than establishing correct PVQ axon guidance (Aurelio et al., 2002; Bülow et al., 2004; Bénard et al., 2006, 2009, 2012; Woo et al., 2008; Pocock et al., 2008), we first investigated when RBR-2 is required for the correct guidance of the PVQs. As shown in Fig. 2A, the aberrant axon guidance occurs in freshly hatched L1 mutant larvae to the same extent as observed at the adult stage, suggesting that RBR-2 is essential for establishing correct axon guidance of the PVQs during embryonic development, but it does not play any role in its maintenance. Second, we investigated in which cells/tissues RBR-2 is required to control PVQ axon guidance. The generation of transgenic lines in which RBR-2::GFP expression is driven by the *rbr-2* promoter showed that RBR-2 is ubiquitously expressed in embryos and larvae (Fig. 2B). Importantly, when expressed in the *rbr-2(tm3141)* mutant, this transgene completely rescued the PVQ defects, further confirming that RBR-2 has a crucial role in axon guidance in these cells (Fig. 2C). To uncover the specificity of the role of *rbr-2* in neuronal development, we re-expressed RBR-2 in the *rbr-2* mutant background using well-characterized tissue-specific promoters, and assayed the transgenic lines for the PVQ phenotypic rescue. These experiments showed that RBR-2 is required specifically in the nervous system (*F25B3.3* promoter), but its presence in hypodermal cells (*dpy-7* promoter) and in muscles (*myo-3* promoter) is not essential (Fig. 2C). The neuronal-specific promoter used in this assay (*F25B3.3* promoter) is active, in the embryos, in four types of neurons, namely PVPs, PVQs, AVKs and embryonic motoneurons (eMNs) (Boulin et al., 2006). As the re-expression of RBR-2 in PVQs (*sra-6* promoter) only partially rescues the PVQ defects observed in *rbr-2* mutants (Fig. 2D), we suggest that RBR-2 acts, to some extent, cell-autonomously, but its expression might be also required in other neuronal cells to ensure correct PVQ axon guidance.

Multiple redundant pathways are known to act in parallel to drive axon guidance and genetic interaction assays have been used to identify their specific components. To test the functional relationship between *rbr-2* and these pathways, we created double mutants carrying *rbr-2(tm3141)* together with mutations of genes acting in axon guidance pathways and measured the penetrance of PVQ defects. As shown in Table S1, we found that *rbr-2* genetically interacts with all the genes tested, suggesting that *rbr-2* acts in concert with the main pathways involved in axon guidance.

### The catalytic activity of RBR-2 is required for correct axon guidance and controls the expression of actin-regulating genes

RBR-2 is the only known H3K4me3/2 demethylase in *C. elegans* (Christensen et al., 2007) and, accordingly, the global level of H3K4me3 is increased in *rbr-2(tm3141)* (Fig. 3A). To investigate whether the enzymatic activity of RBR-2 is required for axon guidance, we performed rescue experiments expressing a catalytically-inactive form of the protein in the *tm3141* genetic background (Fig. 3B; Fig. S2). In contrast to wild-type RBR-2, the mutant protein (called RBR-2DD for Demethylase Dead) was unable to

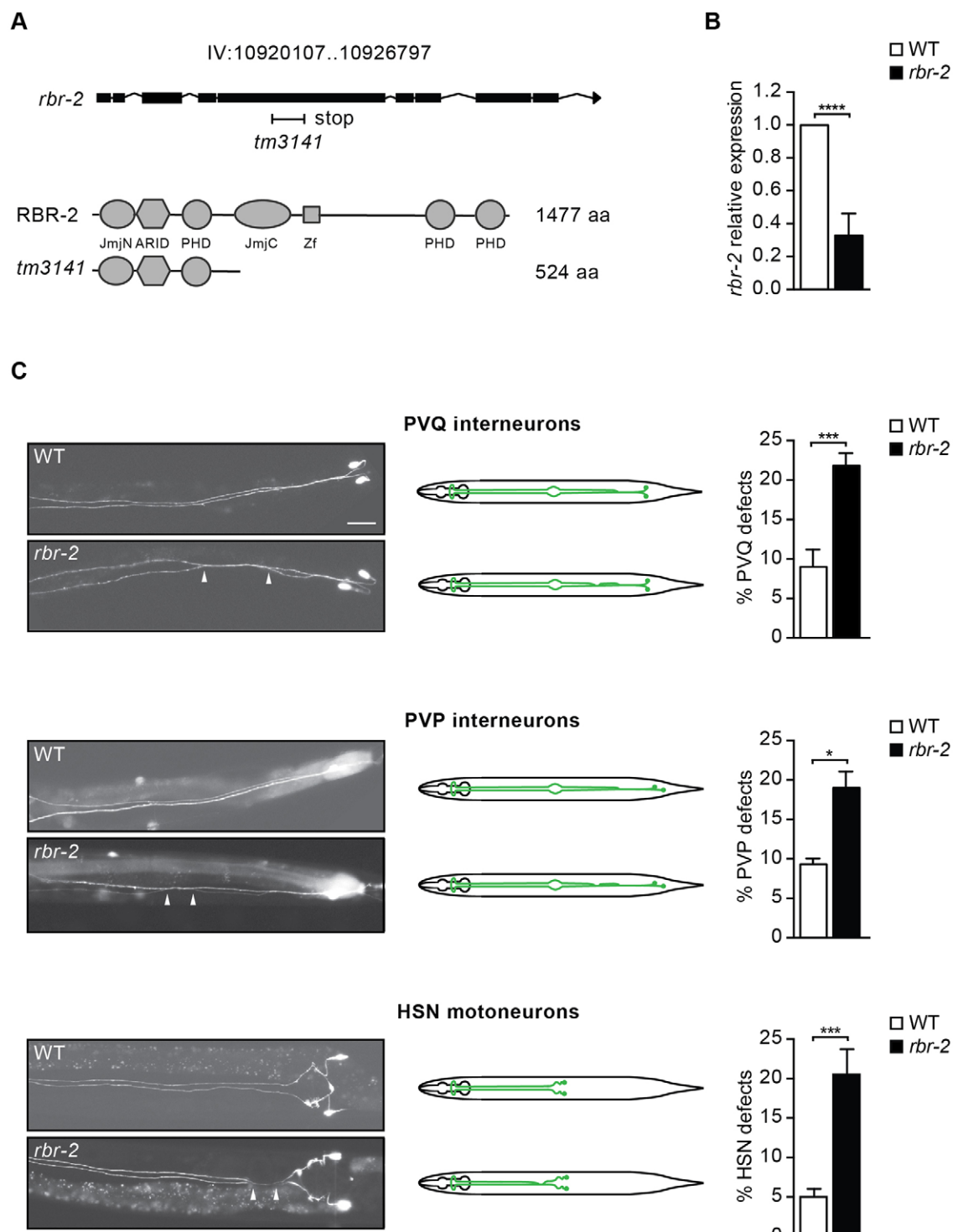


**Fig. 1. RBR-2 is required for correct axon guidance.** (A) Top: Genomic organization of *rbr-2*. Black H-shaped line indicates the position of the *tm3141* deletion. Bottom: RBR-2 and putative *tm3141* protein. JmjN, Jumonji N domain; ARID, AT-rich interacting domain; PHD, plant homeodomain zinc-finger domain; JmjC, Jumonji C domain; Zf, zinc-finger. (B) Greatly reduced *rbr-2* mRNA levels in *rbr-2(tm3141)* embryos, as measured by qPCR using *Y45F10D.4* as internal control. \*\*\*P<0.0001 (Student's t-test). Error bars represent s.e.m. (C) Left: Representative images of PVQ, PVP and HSN neurons in wild-type (WT) and *rbr-2(tm3141)* adult animals, visualized using the transgenes *oyls14*, *hdls26* and *rpEx6*, respectively. Arrowheads indicate the points of axonal cross-over. Ventral view, anterior to the left. Scale bar: 20 µm. Center: Schematics of PVQ, PVP and HSN neurons in wild-type and *rbr-2(tm3141)* animals. Right: Quantification of PVQ, PVP and HSN axonal cross-over defects in *rbr-2(tm3141)* mutant animals. n>100, \*P<0.05, \*\*\*P<0.001 (Fisher's exact test). Error bars represent standard error of proportion.

restore H3K4me3 levels (Fig. 3A) or correct axon guidance of PVQs (Fig. 3B). These results indicate that the catalytic activity of RBR-2 in the removal of the H3K4me3 mark is strictly required for the process of axon guidance.

The genetic interaction assays, showing that *rbr-2* acts in concert with the main pathways implicated in axon guidance, suggest that RBR-2 might interfere with a common downstream effector and/or process. The complex signaling network initiated by guidance cues

**Table 1. Summary of phenotypes in *rbr-2(tm3141)* mutants**

Neurons examined (marker used)	Defective animals (%)	
	WT	<i>rbr-2(tm3141)</i>
Head neurons		
Amphid neurons (Dil)	0	0
Ventral cord neurons		
Interneurons		
AVK interneurons ( <i>bwls2</i> )	2	3
PVP interneurons ( <i>hdls26</i> )	9	19*
PVQ interneurons ( <i>oyls14</i> )	9	22***
Motoneurons		
HSN motoneurons ( <i>rpEx6</i> )		
Axon guidance	5	20***
Cell migration	5	14*
D-type motoneurons ( <i>oxls12</i> )		
Fasciculation ventral nerve cord	6	12
Midline left/right choice	31	35
Fasciculation dorsal nerve cord	0	0
DA/DB motoneurons ( <i>evls82b</i> )		
Midline left/right choice	4	4
DVB motoneuron ( <i>oxls12</i> )	0	0
Tail neurons		
Phasmid neurons (Dil)	0	0

Neurons examined using the indicated transgenic markers. Amphid and phasmid neurons were analyzed using a diffusible dye (Dil). Statistical significance of the difference between wild type and mutants was assessed with Fisher's exact test.  $n>100$ , \* $P<0.05$ , \*\*\* $P<0.001$ .

ultimately regulates, at growth cones, the dynamics of filopodia and lamellipodia, actin-based structures required for axon growth, branching and guidance (Kalil and Dent, 2005; Dent et al., 2011; Chia et al., 2014; Gomez and Letourneau, 2014). The role of WASP, WAVE and Ena/VASP in regulating axon growth and guidance by controlling filopodia formation (Drees and Gertler, 2008; Bear and Gertler, 2009; Tahirovic et al., 2010) is evolutionarily conserved and their *C. elegans* homologs (WSP-1, WVE-1 and UNC-34) are described as the main downstream targets of the signaling pathways regulating axon migration (Fig. 3C) (Shakir et al., 2008; Norris et al., 2009; Mohamed et al., 2012). Therefore, we hypothesized that the aberrant accumulation of H3K4me3 in the *rbr-2* mutant could affect the transcription of actin-regulating genes, leading to the axon guidance defects observed. This hypothesis prompted us to test the role of RBR-2 in regulating the transcription of the three main actin regulators, *wsp-1*, *wve-1* and *unc-34*. First, we measured the expression levels of these genes and found that they were all upregulated in *rbr-2* mutant embryos (Fig. 3D). Second, we investigated whether the overexpression of *wsp-1*, *wve-1* and *unc-34* could result from higher H3K4me3 levels at their TSSs. Indeed, as shown in Fig. 3E, the H3K4me3 levels were increased in the regions surrounding the TSS of all three genes in the *rbr-2* mutant compared with wild-type animals and intergenic regions. Finally, we tested the direct involvement of RBR-2 in H3K4me3 regulation by performing chromatin immunoprecipitation (ChIP)-qPCR with a GFP antibody on chromatin isolated from RBR-2::GFP-expressing worms. RBR-2::GFP was significantly enriched at the TSS of *wsp-1*, *wve-1* and *unc-34*, in comparison with intergenic regions (Fig. 3F). Thus, the catalytic activity of RBR-2 is required for correct axon guidance and for the inhibition of major actin-regulating genes through a mechanism controlling the levels of H3K4me3 at their TSS.

### RBR-2 controls axon guidance by regulating WSP-1 expression

To test whether *wsp-1*, *wve-1* and *unc-34* are key downstream targets of RBR-2 in the regulation of PVQ axon guidance, we used

genetic approaches. We postulated that if the PVQ defects in the *rbr-2* mutant depended on the overexpression of these genes, their removal should ameliorate the phenotype. When *wsp-1* was ablated in the *tm3141* background, we observed a full suppression of the *rbr-2* phenotype (Fig. 4A). By contrast, loss of *wve-1* or *unc-34*, the other two major regulators of actin polymerization, did not improve the PVQ phenotype associated with *rbr-2* deletion (Fig. 4A), demonstrating that WSP-1 is a key component for how RBR-2 regulates axon guidance in these cells.

To investigate further the role of *wsp-1*, we tested whether its overexpression in wild-type animals could reproduce the defects of the *rbr-2* mutant. Indeed, overexpression of WSP-1 in wild-type animals induced the same PVQ defects observed in *rbr-2(tm3141)* (Fig. 4B) and re-expression of WSP-1 in *rbr-2;wsp-1* double mutants also resulted in a significant increase of PVQ defects (Fig. 4C). Importantly, the effect of the increased levels of WSP-1 on PVQ axons was observed only when WSP-1 was overexpressed in neuronal tissue (*F25B3.3* promoter), where we reported the action of RBR-2 in axon guidance (Fig. 4B; Fig. 2C). Collectively, these data show that the increased levels of WSP-1 expression are responsible for the axonal defects in *rbr-2* mutants. In mammals, WASP has been shown to promote F-actin formation through its VCA domain, which interacts directly with the Arp2/3 complex and globular actin and stimulates actin nucleation and branching from existing filaments (Blanchoin et al., 2000; Pantaloni et al., 2000; Amann and Pollard, 2001; Beltzner and Pollard, 2008). Overexpression of the VCA domain leads to excess cellular protrusions in cultured mammalian cells (Yamaguchi et al., 2000) and induces axon guidance defects in *C. elegans* (Shakir et al., 2008). To determine whether the Arp2/3 activation domain was responsible for the *rbr-2* phenotype, we overexpressed the VCA domain in the nervous system using the *F25B3.3* promoter. Interestingly, ectopic expression of the sole VCA domain in wild-type animals mimicked the PVQ axonal cross-overs observed in *rbr-2* mutants (Fig. 4D), strongly suggesting that such defects might arise from abnormal actin dynamics due to increased WSP-1 levels and activity. Moreover, overexpression of the VCA domain in PVQ neurons (*sra-6* promoter) was sufficient to induce the phenotype, further corroborating our hypothesis that RBR-2 could act cell-autonomously (Fig. 4D).

The activity of the mammalian WASP is regulated by a plethora of proteins, of which many are evolutionarily conserved and present in *C. elegans*. Among others, WIP (WIPF1), CDC42 and NCK (NCK1) are known to regulate WASP activity by influencing its conformation and subcellular localization (Rivero-Lezcano et al., 1995; Symons et al., 1996; Abdul-Manan et al., 1999; Martinez-Quiles et al., 2001; Rohatgi et al., 2001; Anton and Jones, 2006; Sawa and Takenawa, 2006). We hypothesized that the removal of their *C. elegans* homologs, WIP-1, CDC-42 and NCK-1, could revert the axonal defects in *rbr-2* worms. Strikingly, loss of *wip-1*, *cdc-42* or *nck-1* resulted in full recovery of the normal PVQ guidance in *rbr-2* mutants (Fig. 4E), further supporting the key role of WSP-1 in regulating this process downstream of RBR-2.

### Role of H3K4me3 readers in axon patterning

Epigenetic regulation of transcription involves proteins that can interpret or 'read' the post-translational modifications of histones (Baker et al., 2008). High levels of H3K4me3 often correlate with transcriptional activation and, in agreement with this, H3K4me3 is involved in the recruitment of ATP-dependent chromatin remodeling factors (Wysocka et al., 2006) and proteins of the basal transcription machinery (Vermeulen et al., 2007). Several

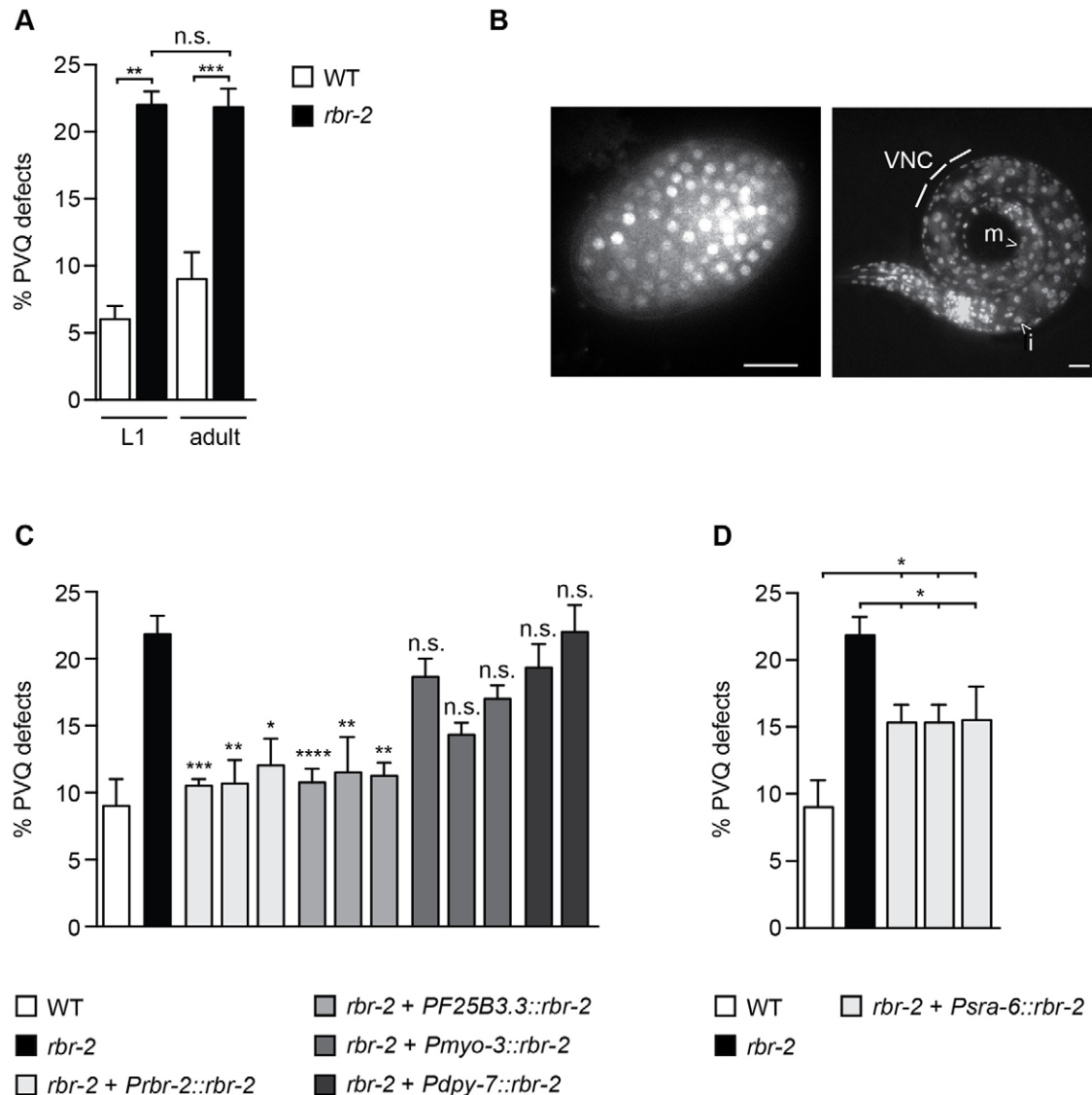


**Fig. 2. RBR-2 is required during embryogenesis in the nervous system to ensure correct axon guidance.** (A) Quantification of PVQ axonal cross-over defects in *rbr-2(tm3141)* mutants at L1 and adult stages.  $n > 100$ , \*\* $P < 0.01$ , \*\*\* $P < 0.001$ , n.s., not significant (one-way ANOVA followed by Tukey's multiple-comparison test). (B) Expression of the *Prbr-2::rbr-2::GFP* translational reporter at embryonic and larval stages. Ventral nerve cord (VNC), muscle (m) and intestinal cells (i) are indicated. Anterior to the left. Scale bars: 10  $\mu$ m. (C,D) Tissue- (C) and cell-specific (D) rescue analyses. Promoters used for transgenic rescue are: *PF25B3.3*, nervous system; *Pmyo-3*, body-wall muscles; *Pdpy-7*, hypodermis; *Psra-6*, PVQs. Statistical significance was calculated in relation to non-transgenic controls (values not shown) for each transgenic line.  $n > 100$ , \* $P < 0.05$ , \*\* $P < 0.01$ , \*\*\* $P < 0.001$ , n.s., not significant (one-way ANOVA followed by Tukey's multiple-comparison test). At least two independent lines for each transgene were analyzed. Error bars represent standard error of proportion.

reports have illustrated that H3K4me3 can be specifically recognized by proteins with a PHD zinc-finger domain (Musselman and Kutateladze, 2011), including the recombination activating gene RAG2, the large subunit of the nucleosome remodeling factor complex (NURF) BPTF, the inhibitor of growth ING2, the TAF3 subunit of TFID (TBP) and the KDM7 family members PHF2/8 and KIAA1718 (KDM7A) (Badenhorst et al., 2002; Li et al., 2006; Peña et al., 2006; Shi et al., 2006; Wysocka et al., 2006; Matthews et al., 2007; Vermeulen et al., 2007; Palacios et al., 2008; Kleine-Kohlbrenner et al., 2010; Fortschegger and Shiekhattar, 2011). These PHD-containing proteins, except RAG2, are all conserved in *C. elegans* and viable mutant alleles are available for most of them (Table S2). We hypothesized that in the *rbr-2* mutant the increased levels of H3K4me3 could be interpreted by one or more H3K4me3 readers, leading to inappropriate

transcriptional activation of *wsp-1*. If this were the case, genetic ablation of the specific reader(s) in the *rbr-2* background should rescue the PVQ axon guidance phenotype. We found that the removal of *nurf-1* (homolog of BPTF), but not of *ing-3*, *jmjd-1.1/1.2* and *isy-13*, significantly ameliorated the *rbr-2* phenotype (Fig. 5A; Table S3), suggesting that NURF-1 is responsible for sensing and interpreting the increased levels of H3K4me3 in the *rbr-2* mutant. Accordingly, loss of *isw-1*, homolog of the catalytic component of the NURF complex ISWI, also fully suppressed the *rbr-2* axonal defects (Fig. 5B). Importantly, the level of *wsp-1* mRNA was significantly reduced and resumed wild-type expression in *rbr-2;nurf-1* and *rbr-2;isw-1* double mutants in comparison with *rbr-2* alone (Fig. 5C). These results strongly suggest that NURF-1 and ISW-1 are required for the inappropriate activation of *wsp-1* transcription that occurs in the absence of *rbr-2*.

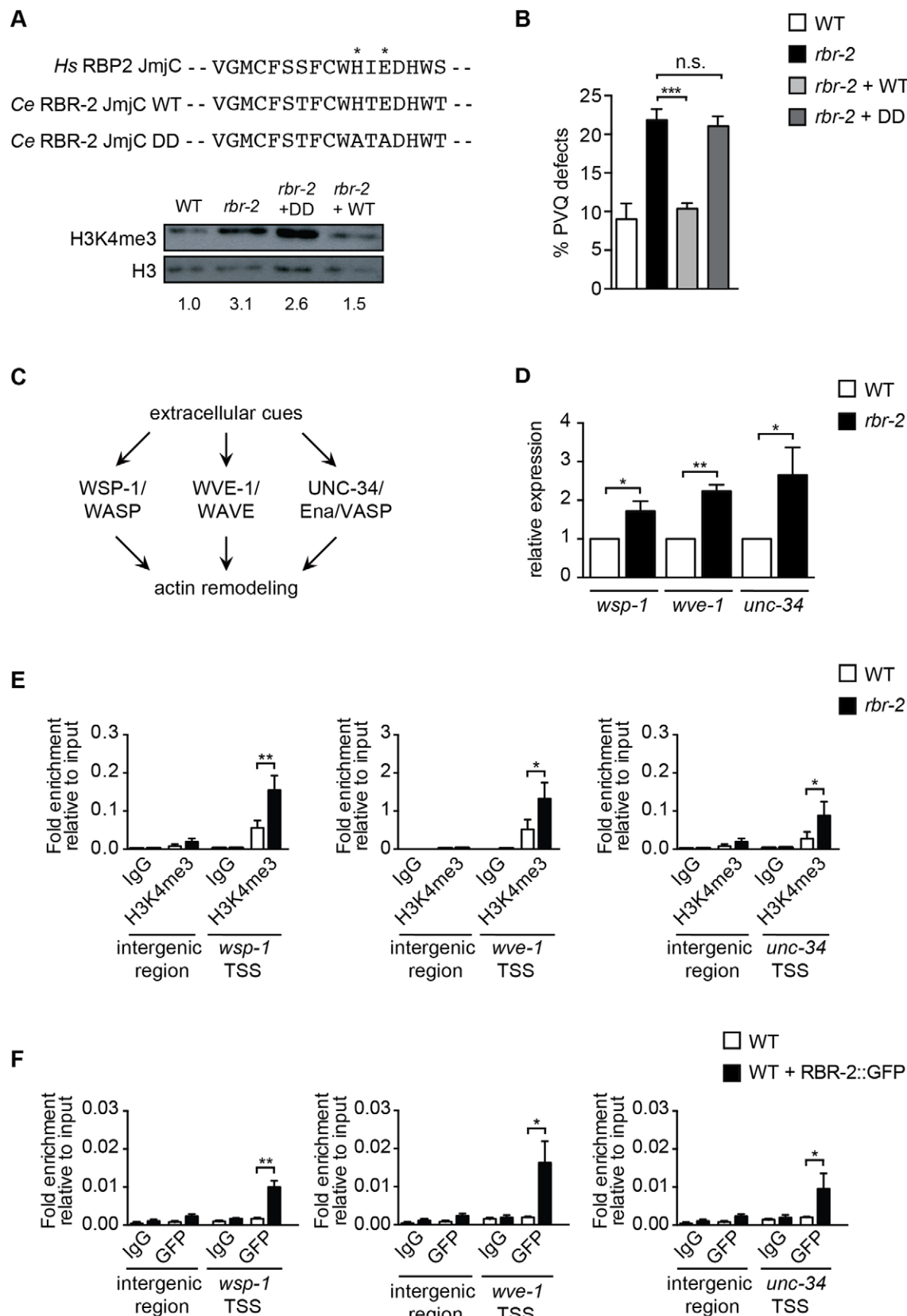


Fig. 3. See next page for legend.

**DISCUSSION**

In this study, we show that the unique member of the KDM5 class of H3K4me3/2 demethylase RBR-2 is required for correct axon

guidance in *C. elegans* through a mechanism involving the transcriptional regulation of *wsp-1*. Loss of RBR-2 leads to increased levels of H3K4me3 at the TSS of *wsp-1* and

**Fig. 3. RBR-2 modulates the expression of proteins regulating actin dynamics.** (A) Top: Alignment of a part of the Jumonji C domain of human RBP2 with wild-type (WT) RBR-2 and with the catalytically inactive RBR-2DD (DD, Demethylase Dead). Asterisks mark two conserved amino acids in the iron-binding domain (HxD/EX<sub>n</sub>H) of the JmjC domain, modified in the RBR-2DD. Bottom: Quantified levels (relative to WT) of H3K4me3 in wild-type, *rbr-2(tm3141)* and *rbr-2(tm3141)* animals carrying a translational GFP fusion of catalytically inactive RBR-2 (*rbr-2+DD*) or wild-type RBR-2 (*rbr-2+WT*). H3 is used as loading control. (B) Quantification of PVQ axonal cross-over defects in *rbr-2(tm3141)* expressing a translational construct encoding for wild-type (*rbr-2+WT*) and catalytically inactive (*rbr-2+DD*) RBR-2. Data are representative of three independent lines for each transgene and statistical significance was calculated in relation to non-transgenic controls for each transgenic line.  $n=100$ , \*\*\* $P<0.001$ , n.s., not significant (one-way ANOVA followed by Tukey's multiple-comparison test). Error bars represent standard error of proportion. (C) WSP-1/WASP, WVE-1/WAVE and UNC-34/Ena/VASP integrate multiple signalling pathways to regulate actin dynamics. (D) mRNA levels of *wsp-1*, *wve-1* and *unc-34* in *rbr-2(tm3141)* embryos as measured by qPCR, using *pmp-3* as internal control. (E) ChIP-qPCR assay for H3K4me3 on *wsp-1*, *wve-1* and *unc-34* TSS and intergenic regions in wild-type and *rbr-2(tm3141)* embryos. ChIPs with antibody against IgG served as negative controls. ChIP enrichments are normalized to input. (F) ChIP-qPCR assay for GFP on *wsp-1*, *wve-1* and *unc-34* TSS and intergenic regions in wild-type embryos carrying a translational GFP fusion of RBR-2 (WT+RBR-2::GFP). ChIPs with antibody against IgG served as negative controls. ChIP enrichments are normalized to input. In D-F, data are the average of three biological independent experiments and are expressed as mean±s.e.m.; \* $P<0.05$ , \*\* $P<0.01$  (Student's *t*-test).

concomitant upregulation of its transcription, resulting in axonal defects. Furthermore, we show that the NURF complex is required for *wsp-1* upregulation in the *rbr-2* mutant and thus for translating the increased H3K4me3 signal into aberrant axon guidance.

Our analysis indicates that RBR-2 is required throughout development, as it functions in neurons that mature during embryonic (PVPs, PVQs) and postembryonic (HSNs) development. Projections of other neurons are unaffected in the *rbr-2(tm3141)* mutant. Thus, the function of *rbr-2* appears to be restricted to a subset of neurons and its loss has a limited effect on global neuronal architecture. Genetic interaction assays suggest that RBR-2 acts in the most common pathways known to guide axon migration. The simplest explanation for this result is that the action of RBR-2 is required for regulating downstream targets of these pathways and cytoskeletal proteins are therefore potential candidates.

Using genetic and molecular approaches we identified WSP-1, an activator of the actin-nucleating complex Arp2/3, as a key protein required for the misguidance of PVQ axons in *rbr-2* mutant worms. Briefly, we have demonstrated that: (1) RBR-2 is enriched at the *wsp-1* promoter; (2) loss of *rbr-2* results in increased levels of H3K4me3 at the *wsp-1* TSS, in association with its transcriptional upregulation; (3) loss of *wsp-1* in *rbr-2* mutants fully restores normal PVQ axon guidance; (4) the overexpression of WSP-1 or its VCA domain lead to axon guidance defects similar to those observed in *rbr-2(tm3141)*; and (5) inactivation of genes that encode proteins required for WSP-1 stability, localization and activation suppresses the *rbr-2* mutant PVQ phenotype. The effect of loss of *rbr-2* on the expression of *wsp-1* is rather modest, as expected considering the cell-specific action of *rbr-2* and the fact that we use full embryos to analyze the levels of *wsp-1*. Based on the well-established role of WSP-1 mammalian homologs, WASP/N-WASP, in positively regulating filopodia formation (Symons et al., 1996; Miki et al., 1998; Castellano et al., 1999; Kessels et al., 2011), we suggest that the upregulation of WSP-1 in *C. elegans* might lead to misregulated filopodia dynamics at the growth cone of the PVQ axons and to an aberrant response to different extracellular signals.

This hypothesis is corroborated by tissue-specific rescue experiments, pointing to a cell-autonomous role of RBR-2 and WSP-1 in the PVQs.

The identification of actin-remodeling genes as targets of RBR-2 is interesting in the context of neurological disorders. The H3K4me3 demethylase KDM5C is mutated in X-linked mental retardation (Iwase et al., 2007; Abidi et al., 2008; Adegbola et al., 2008; Gonçalves et al., 2014). Further, mutations in *KDM5B* have been reported in individuals with non-syndromic intellectual disability and autism spectrum disorders (Athanasakis et al., 2014; De Rubeis et al., 2014; Iossifov et al., 2014) and mutations in *KDM5A* have been linked to an autosomal recessive form of intellectual disability (Najmabadi et al., 2011). Similarly, several genes implicated in cytoskeleton dynamics are mutated in intellectual disability and autism spectrum disorders (Nadif Kasri and Van Aelst, 2008; Ba et al., 2013; Hu et al., 2014; Srivastava and Schwartz, 2014). Thus, our results help to establish a functional link between chromatin regulators and the actin-remodeling genes required for axon/dendrite formation and synaptic plasticity, which are processes compromised in neurodevelopmental and psychiatric disorders. However, considering the complexity underpinning intellectual disability disorders, it is possible that distinct mechanisms might act in cell-specific manners. Indeed, although ectopic expression of RBR-2 is able to rescue the axon migration defects of another pair of neurons (HSNs) observed in the *rbr-2* mutant, loss of *wsp-1* is not (Fig. S3), suggesting that RBR-2 might control axon guidance through different molecules/mechanisms. Thus, future analyses will be needed to molecularly dissect RBR-2 functions in other neuronal contexts.

Rescue analysis indicates that the H3K4me3 demethylase activity of RBR-2 is required for achieving correct axon guidance, providing a strong link between misregulated H3K4 methylation levels and the axonal phenotype. Several proteins, including those containing the evolutionarily conserved PHD domain, are known to bind specifically to H3K4me3, thereby translating the methylation status into a cellular process (reviewed by Sims and Reinberg, 2006; Vermeulen and Timmers, 2010). We showed that inactivation of *nurf-1*, coding for the large subunit of the NURF nucleosome-remodeling complex, reverts the *rbr-2* phenotype. Consistently, the genetic ablation of *isw-1*, homolog of the ISWI catalytic component of the NURF complex, results in a similar outcome. In mammals, the NURF complex is recruited to chromatin through the interaction of its PHD domain with H3K4me3 where it catalyzes ATP-dependent nucleosome sliding at core promoters, facilitating transcription both *in vitro* and *in vivo* (Mizuguchi et al., 1997; Barak et al., 2003). Interestingly, the NURF complex is known to regulate some aspects of neuronal development (Lazzaro and Picketts, 2001; Barak et al., 2003), including neurite outgrowth (Barak et al., 2003). Thus, based on our results, we propose a model (Fig. 5D) in which increased levels of H3K4me3 at promoter regions occurring in the absence of RBR-2 could result in recruitment of the NURF complex to RBR-2 target genes, e.g. *wsp-1*, leading to changes in chromatin structure that favor transcription. In turn, increased levels of WSP-1 result in aberrant actin dynamics and axon guidance. The lack of a specific antibody against NURF-1 has prevented us from directly demonstrating increased levels of NURF-1 binding to RBR-2-regulated promoters in the *rbr-2* mutant. However, the fact that inactivation of *nurf-1* in *rbr-2* mutant worms is accompanied by a reduction of *wsp-1* expression to wild-type levels and by re-establishment of normal axon guidance strongly suggest that NURF-1 contributes to the overexpression of *wsp-1* by binding to H3K4me3 at the TSS of *wsp-1*.

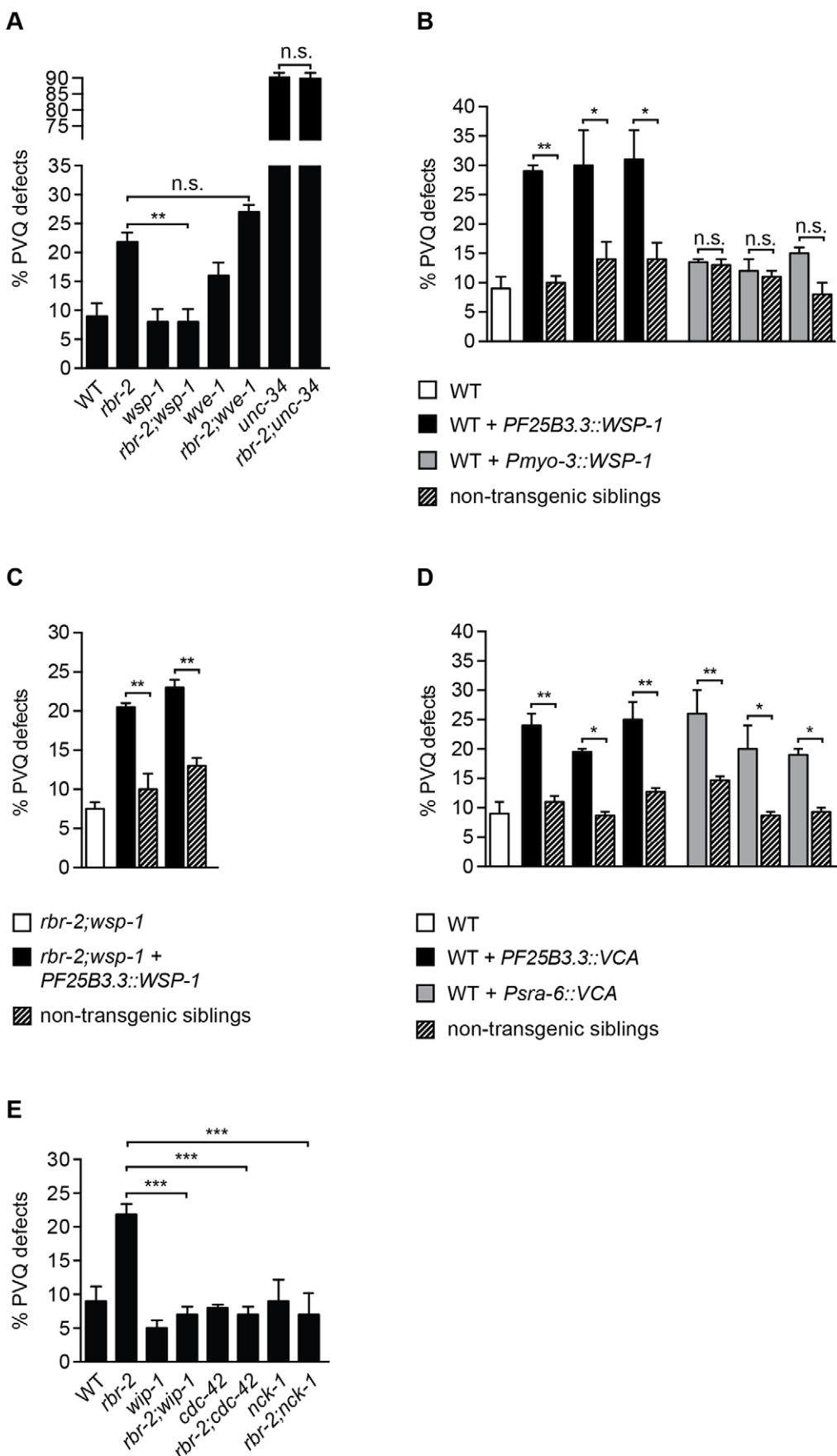


Fig. 4. See next page for legend.

**Fig. 4. RBR-2 controls axon guidance by regulating WSP-1 levels.**

(A) Quantification of PVQ axonal cross-over defects in *rbr-2(tm3141)* and double mutants with actin regulators *wsp-1(gm324)*, *wve-1(ok3308)* and *unc-34(e566)*.  $n>100$ , \*\* $P<0.01$ , n.s., not significant (one-way ANOVA followed by Tukey's multiple-comparison test). (B) Quantification of PVQ axonal cross-over defects in wild-type (WT) animals carrying a translational construct for WSP-1 expressed under the control of a neuronal (*PF25B3.3*) or a muscular (*Pmyo-3*) promoter.  $n=100$ , \* $P<0.05$ , \*\* $P<0.01$ , n.s. not significant (one-way ANOVA followed by Tukey's multiple-comparison test). Three independent lines for each transgene were analyzed. (C) Quantification of PVQ axonal cross-over defects in *rbr-2(tm3141);wsp-1(gm324)* animals carrying a translational construct for WSP-1 expressed under the control of a neuronal promoter (*PF25B3.3*).  $n=100$ , \*\* $P<0.01$  (one-way ANOVA followed by Tukey's multiple-comparison test). Two independent lines were analyzed. (D) Quantification of PVQ axonal cross-over defects in wild-type animals carrying a translational construct for the VCA Arp2/3 activation domain of WSP-1 expressed under the control of a neuronal (*PF25B3.3*) or a PVQ-specific (*Psra-6*) promoter.  $n=100$ , \* $P<0.05$ , \*\* $P<0.01$  (one-way ANOVA followed by Tukey's multiple-comparison test). Three independent lines for each transgene were analyzed. (E) Quantification of PVQ axonal cross-over defects in *rbr-2(tm3141)* and double mutants with WSP-1 regulators *wip-1(ok2435)*, *cdc-42(gk388)* and *nck-1(ok694)*.  $n>100$ , \*\*\* $P<0.001$  (one-way ANOVA followed by Tukey's multiple-comparison test). Error bars represent standard error of proportion.

In conclusion, our study establishes a precise role for epigenetic regulation in neuronal development by connecting the catalytic activity of RBR-2 to H3K4me3 levels and the NURF complex in controlling WSP-1 transcription. Future work will be aimed at identifying the molecules required for the cell-specific action of RBR-2 and the neuronal functions of other H3K4 regulators mutated in intellectual disability syndromes, with the hope of providing mechanistic insights that may be relevant for developing therapeutic treatments.

**MATERIALS AND METHODS****Genetics and strains**

*C. elegans* strains were cultured using standard growth conditions at 20°C on *Escherichia coli* OP50 (Brenner, 1974). Strains used were as follows: wild type Bristol: N2; *rbr-2(tm3141)* IV; *rbr-2(tm1231)* IV; CX5334: *oyIs14* {[*Psra-6::GFP*]+lin-15(+)} V; lin-15(n765) X; VH648: *hdls26*(*Podr-2::CFP*; *Psra-6::DsRed2*) III; MU1085: *bwlIs2*[*Pflp-1::GFP*]+(*pRF4*)rol-6 (su1006) J; EG1285: *oxlIs12*{[*Punc-47::GFP*]+lin-15(+)} X; lin-15(n765) X; NW1100: *evlIs82b*{[*Punc-129::GFP*]+*dpy-20(+)*} IV; *dpy-20(e1282)* IV; HT1593: *unc-119(ed3)* III; NG324: *wsp-1(gm324)* IV; VC2706: *wve-1(ok3308)* I/hT2[bli-4(e937)]; *let-?(q782)*; *qls48* (I;III); CB566: *unc-34(e566)* V; VC2053: *wip-1(ok2435)* III/hT2[bli-4(e937)]; *let-?(q782)*; *qls48* (I;III); VC898: *cdc-42(gk388)/mIn1/mIs14*; *dpy-10(e128)* II; RB860: *nck-1(ok694)* X; MT13649: *nurf-1(n4295)* II; *ing-3(tm2530)* II; RB1343: *T06A10.4/ksy-13(ok1475)* IV; *jmd-1.1(tm3980)* II; *jmd-1.2(tm3713)* IV; MT15795: *isw-1(n3294)* III; CX3198: *sax-3(ky123)* X; CX5000: *slt-1(eh15)* X; OH4139: [*vab-1(dx31)* II; *oyIs14*]; CZ4111: *vab-2(ju1)* IV; NW1549: *efn-2(ev658);efn-3(ev696)* X; OH1487: *hse-5(tm472)* III; AH205: *sdn-1(zh20)* X; NW1700: [*plx-2(ev773)* II; *him-5(e1490)* V]. The strains *rpEx6(Pph-1::GFP*; *Psra-6::RFP*) and *unc-5(e53)* IV were generous gifts from Roger Pocock (Department of Anatomy and Developmental Biology, Monash University, Melbourne, VIC, Australia). Double mutant animals with specific genetic backgrounds were generated by standard crossing procedure. For a complete list of the transgenic strains generated for this study, see Table S4.

***rbr-2* alleles**

The allele *rbr-2(tm3141)* carries a deletion of 365 bp and an insertion of 8 bp, leading to a frameshift and a premature stop codon. The predicted protein, if translated, contains only the N-terminal portion of RBR-2, until the first PHD domain (Fig. 1A). The *C. elegans* mutant strain *rbr-2(tm1231)* carries an in-frame-deletion of 648 bp and the putative mutant transcript can give rise to a protein of 1261 amino acids lacking the JmjC domain (Fig. S1B). The alleles *tm3141* and *tm1231* were

identified by the National BioResource Project (NBRP), Japan, and were backcrossed at least three times with wild-type animals before phenotypic analyses.

**Generation of transgenic constructs**

For the *rbr-2::GFP* construct, a 6081-bp fragment of *rbr-2* (ZK593.4 in WormBase) containing the entire coding region and a 2540-bp promoter region were PCR-amplified from N2 genomic DNA. The resulting fragments were inserted in the multiple cloning sites of the pDONR pCR8 and the pDONR P4-P1R vectors, respectively (Gateway Cloning System, Life Technologies). The *rbr-2* genomic sequence was amplified with the primers *rbr-2\_Fw* (ATCGCTGCACGTGTCAGA) and *rbr-2\_Rv* (ATCGGTGGAAACACTCGAA) and the primers *prom\_rbr-2\_Fw* (GGGGACAACTTGTATAGAAAAGTTGaatacttttgtgtttt) and *prom\_rbr-2\_Rv* (GGGGACTGCTTTGTACAAACTTGTttttcgtttggc-tt) were used to amplify the *rbr-2* promoter region.

Plasmids were constructed using MultiSite Gateway Three-Fragment Vector Construction Kit (Life Technologies). Tissue-specific promoters were cloned into the pDONR P4-P1R vector. The pDONR P2-RP3 vector containing the *GFP* sequence followed by *unc-54* 3'UTR was a generous gift from Erik Jorgensen (Department of Biology, University of Utah, Salt Lake City, UT, USA). Final constructs were cloned into the pDEST R4-R3 destination vector.

To generate an integrated line, the vectors pDONR P4-P1R [*Prbr-2*], pDONR pCR8 [*rbr-2*] and pDONR P2-RP3 [*GFP::unc-54* 3'UTR] were recombined with the destination vector pCG150 (Addgene), which includes the *unc-119* rescue fragment into the vector backbone pDEST R4-R3.

For the *rbr-2DD::GFP* construct, the *rbr-2::GFP* construct was mutated using the QuikChange Site-Directed Mutagenesis Kit (Stratagene). Specifically, the DNA sequence was mutated so that the histidine at position 514 (H514) and the glutamic acid at position 516 (E516) were changed to alanine. Primers *rbr-2\_H514E516A\_Fw2* (GTTCTGCTGGGCCACCGCGGATATTGGAC) and *rbr-2\_H514E516A\_Rv2* (GTCCAA-TGATCCGCGGTGGCCCAGCAGAAC) were used for the site-directed mutagenesis to generate the *rbr-2* catalytic dead mutant construct.

The vectors pJZ4 [*PF25B3.3::wsp-1a cDNA*] and pJZ3 [*Pmyo-3::wsp-1a cDNA*] were generous gifts from Terry Kubisesky (Department of Biology, York University, Toronto, ON, Canada).

The cDNA encoding the VCA domain of WSP-1 [9108-9579 of the *wsp-1* gene (*C07G1.4a* in WormBase)] was PCR-amplified from pJZ4 with the primers *VCA\_GW\_fw* (aaacatatTCAGGAGCCGGAGGACCT) and *VCA\_GW\_rv* (ATCTGACCATTCACTTTGTCAT). Of note, the *wsp-1* initiator methionine and six upstream nucleotides were included in the forward PCR primer upstream of the VCA region, as described by Shakir et al. (2008). The resulting fragment was inserted in the multiple cloning site of the pDONR pCR8 vector and the final plasmids expressing *PF25B3.3::VCA cDNA::GFP* and *Psra-6::VCA cDNA::GFP* were constructed using MultiSite Gateway Three-Fragment Vector Construction Kit.

The DNA sequences of all constructs were verified by sequencing.

**Microinjection and production of transgenic lines**

Transgenic lines were obtained through microinjection (Mello et al., 1991). Constructs were injected into young adult hermaphrodites as extrachromosomal arrays at 10–50 ng  $\mu\text{l}^{-1}$  with *Ptx-3::RFP* (50–90 ng  $\mu\text{l}^{-1}$ ) or *Pmyo-2::mCherry* (0.5–5 ng  $\mu\text{l}^{-1}$ ) as injection markers. To obtain an integrated line, 20 ng  $\mu\text{l}^{-1}$  of the vector pCG150 [*Prbr-2::rbr-2::GFP::unc-54* 3'UTR] [*unc-119*] were injected in [*unc-119(ed3)*] genetic background, integrated by UV irradiation and backcrossed three times with N2 before analyses.

**Fluorescence microscopy**

Neuronal phenotypes were scored in young adult hermaphrodites grown at 25°C. The PVQ and HSN neurons were visualized using the transgenes *oyIs14* and *rpEx6*, respectively. In Fig. 2C and Fig. 3B, the transgene *hdls26*, which allows the simultaneous visualization of PVPs and PVQs, was used in some lines. Of note, the distribution of PVQ defects between wild type and *rbr-2* mutants was similar in either *oyIs14* or *hdls26* backgrounds. Images were taken using an automated fluorescence microscope (Zeiss, AXIO

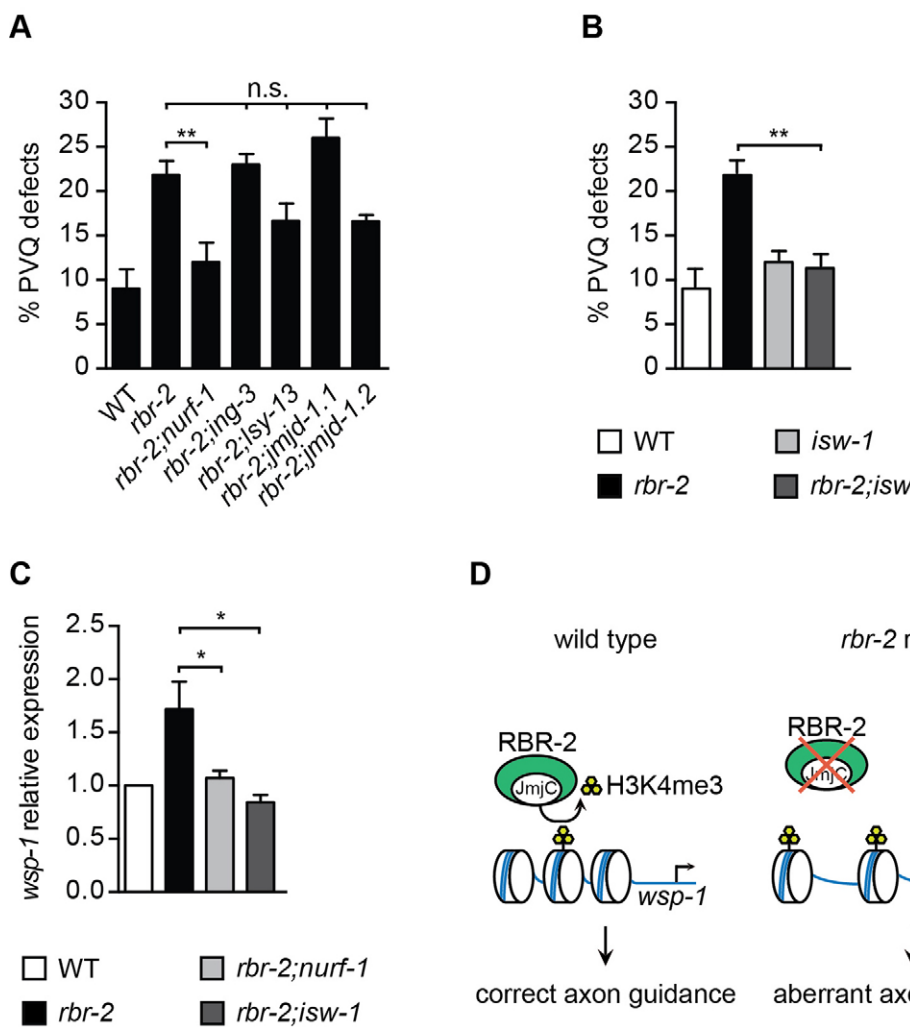


**Fig. 5. Loss of the NURF complex rescues the PVQ axonal cross-over defects associated with *rbr-2*(*tm3141*) and restores correct level of *wsp-1* mRNA.** (A) Quantification of PVQ axonal cross-over defects in *rbr-2*(*tm3141*) and double mutants with PHD-containing proteins *nurf-1*(*n4295*), *ing-3*(*tm2530*), *isy-13* (*ok1475*), *jmjd-1.1*(*tm3980*) and *jmjd-1.2*(*tm3713*).  $n>100$ , \*\* $P<0.01$ , n.s., not significant (one-way ANOVA followed by Tukey's multiple-comparison test). Error bars represent standard error of proportion. (B) Quantification of PVQ axonal cross-over defects in *rbr-2*(*tm3141*), *isw-1*(*n3294*) and double mutant.  $n>100$ , \*\* $P<0.01$  (one-way ANOVA followed by Tukey's multiple-comparison test). Error bars represent standard error of proportion. (C) mRNA levels of *wsp-1* in *rbr-2*(*tm3141*), *rbr-2*(*tm3141*);*nurf-1*(*n4295*) and *rbr-2*(*tm3141*);*isw-1*(*n3294*) embryos as measured by qPCR, using *pmp-3* as internal control. Data are the average of three biological independent experiments and are expressed as mean±s.e.m. \* $P<0.05$  (Student's *t*-test). (D) Model of the mechanism of action of RBR-2 as a negative regulator of *wsp-1* transcription. In wild type, RBR-2 regulates the level of H3K4me3 at *wsp-1* TSS and secures correct axon guidance. Loss of *rbr-2* leads to increased levels of H3K4me3 and of NURF complex recruitment at *wsp-1* TSS and consequently to overexpression of WSP-1, resulting in aberrant actin remodeling and axon guidance.

Imager M2) and MicroManager software (version 1.4.11). All pictures were exported in preparation for printing using Photoshop (Adobe).

#### Dil staining of amphid and phasmid neurons

Young adult hermaphrodites cultured at 25°C were transferred from a plate into an eppendorf tube with 1 ml M9, spun down at 1500 g and washed twice. Worms were resuspended in 1 ml M9 and 5 µl were added from a stock dye solution containing 2 mg ml<sup>-1</sup> Dil (Molecular Probes, catalog # D-282) in dimethyl formamide. Eppendorf tubes were incubated wrapped in foil on a slow shaker for 3 h. Worms were spun down at 1500 g and washed twice with M9 before being analyzed by fluorescence microscopy using the Texas Red filter, as described above.

#### Chromatin immunoprecipitation (ChIP)

Gravid hermaphrodites cultured at 25°C were treated with hypochlorite solution and embryos were flash-frozen in liquid nitrogen and stored at -80°C before chromatin immunoprecipitation. ChIP was performed with a protocol

modified from that of Kolasinska-Zwierz et al. (2009). Chromatin was disrupted by sonication using a Diagenode Bioruptor sonicator UCD-300 to obtain fragments of 200-500 bp in size. Suitable amounts of chromatin were incubated with the following antibodies overnight: polyclonal anti-H3K4me3 (Abcam, ab8580; 1:1000), polyclonal anti-IgG (Sigma, I8140; 1:1000), polyclonal anti-GFP (Abcam, ab290; 1:500). Immunoprecipitated complexes were recovered on magnetic Protein G Dynabeads (Invitrogen) and, after extensive washes, DNA was isolated by reverse cross-linking and purification using the QIAquick PCR Purification Kit (Qiagen). For ChIP-qPCR, immunoprecipitated DNA and input were quantified by real-time qPCR as described below. The measures were normalized to the input. All reactions were performed in duplicate, in three independent experiments.

#### Real-time quantitative PCR (RT-qPCR)

Late embryos were obtained by hypochlorite treatment of gravid hermaphrodites followed by 6-8 h of suspension of the embryos in M9 at room temperature. Embryos were flash-frozen in liquid nitrogen and stored at

–80°C before RNA extraction. Total RNA was isolated using TRIzol reagent (Life Technologies) and the RNeasy Mini Kit (Qiagen). cDNA was synthesized using oligo(dT)<sub>16</sub> primers and reagents from the TaqMan Reverse Transcription Kit (Applied Biosystems). qPCR was performed using Maxima SYBR Green/ROX qPCR Master Mix 2× (Thermo Scientific) on a LightCycler480 Real-Time PCR System (Roche). The measures were normalized to *pmp-3* and *Y45F10D.4* RNA levels, which have been reported to be unusually stable (Zhang et al., 2012), with similar results. All reactions were performed in duplicate, in three independent experiments.

### Western blot analysis

Total protein extracts were prepared from L4 hermaphrodites grown on OP50 at 25°C. Protein concentration was estimated using the modified micro-Lowry assay and equal amounts of protein were loaded. The following antibodies were used: polyclonal anti-H3K4me3 (Abcam, ab8580, lot GR152455-1; 1:5000); polyclonal anti-H3 (Abcam, ab1791, lot GR9204-1; 1:30,000); peroxidase-labeled anti-rabbit secondary antibody (Vector; 1:10,000). Western blots were quantified using the ImageJ program (National Institutes of Health).

### Statistical analyses

All phenotypes were scored as percentages of defective animals and results are shown with error bars representing the standard error of proportion. Statistical analyses were performed in GraphPad Prism 6 using Fisher's exact test, for pairwise comparisons, or one-way ANOVA followed by Tukey's test, for multiple comparisons. In rescue and overexpression experiments, significance was calculated in relation to non-transgenic controls for each transgenic line. As the penetrance of defects in non-transgenic siblings was always consistent with the phenotype of *rbr-2(tm3141)*, these data are not shown in Fig. 2C,D and Fig. 3B.

qPCR data are expressed as mean±s.e.m. and compared using Student's *t*-test. Differences with a *P*-value <0.05 were considered significant.

### Acknowledgements

We thank the *Caenorhabditis* Genetics Center (CGC), the National BioResource project for *C. elegans* (Japan) and the international *C. elegans* Gene Knockout Consortium for providing strains. We are grateful to Roger Pocock for strains and discussion; Kristian Helin for critical reading of the manuscript; Erik Jorgensen and Terry Kubishevsky for providing vectors; Giorgio Galli for advice regarding ChIP analyses; and Alexandra Avram for technical assistance.

### Competing interests

The authors declare no competing or financial interests.

### Author contributions

L.M. carried out all the experimental work with the contribution of Y.C.L., J.V. and A.R. A.E.S and L.M. designed the experiments, analyzed the data and wrote the manuscript.

### Funding

This work was supported by a grant from the Danish National Research Foundation [DNRF82 to A.E.S.].

### Supplementary information

Supplementary information available online at <http://dev.biologists.org/lookup/suppl/doi:10.1242/dev.132985/-DC1>

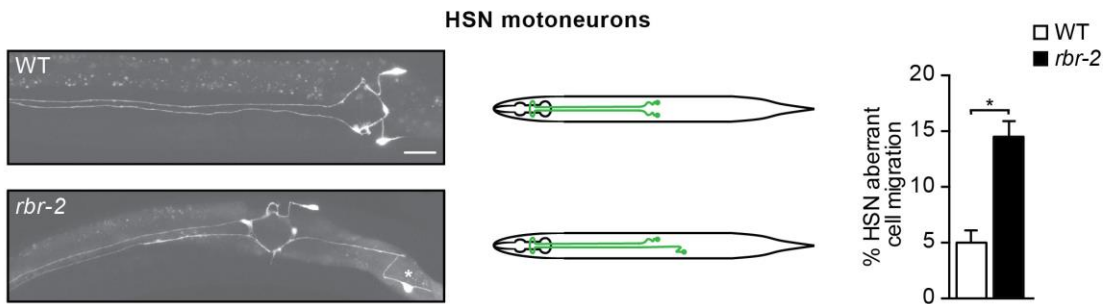
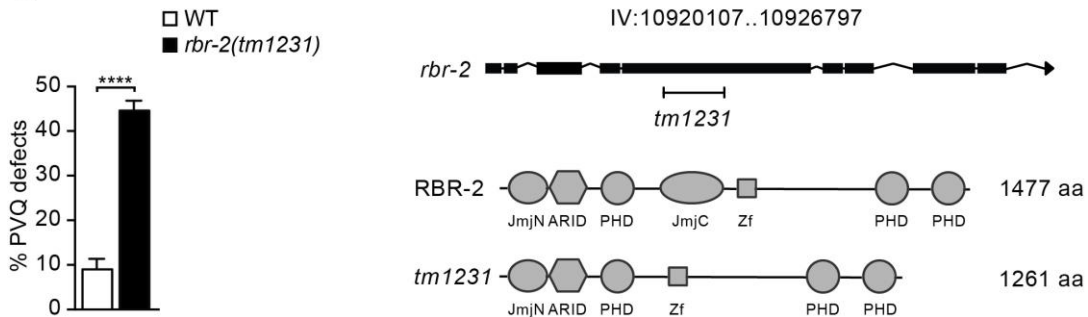
### References

- Abdul-Manan, N., Aghazadeh, B., Liu, G. A., Majumdar, A., Ouerfelli, O., Siminovitch, K. A. and Rosen, M. K. (1999). Structure of Cdc42 in complex with the GTPase-binding domain of the 'Wiskott-Aldrich syndrome' protein. *Nature* **399**, 379–383.
- Abidi, F. E., Holloway, L., Moore, C. A., Weaver, D. D., Simensen, R. J., Stevenson, R. E., Rogers, R. C. and Schwartz, C. E. (2008). Mutations in JARID1C are associated with X-linked mental retardation, short stature and hyperreflexia. *J. Med. Genet.* **45**, 787–793.
- Adegbola, A., Gao, H., Sommer, S. and Browning, M. (2008). A novel mutation in JARID1C/SMCX in a patient with autism spectrum disorder (ASD). *Am. J. Med. Genet. A* **146A**, 505–511.
- Albert, M., Schmitz, S. U., Kooistra, S. M., Malatesta, M., Morales Torres, C., Rekling, J. C., Johansen, J. V., Abarrategui, I. and Helin, K. (2013). The histone demethylase Jarid1b ensures faithful mouse development by protecting developmental genes from aberrant H3K4me3. *PLoS Genet.* **9**, e1003461.
- Amann, K. J. and Pollard, T. D. (2001). The Arp2/3 complex nucleates actin filament branches from the sides of pre-existing filaments. *Nat. Cell Biol.* **3**, 306–310.
- Anton, I. M. and Jones, G. E. (2006). WIP: a multifunctional protein involved in actin cytoskeleton regulation. *Eur. J. Cell Biol.* **85**, 295–304.
- Athanasakis, E., Licastro, D., Faletta, F., Fabbretto, A., Dipresa, S., Vozzi, D., Morgan, A., d'Adamo, A. P., Pecile, V., Biarnés, X. et al. (2014). Next generation sequencing in nonsyndromic intellectual disability: from a negative molecular karyotype to a possible causative mutation detection. *Am. J. Med. Genet. A* **164**, 170–176.
- Aurelio, O., Hall, D. H. and Hobert, O. (2002). Immunoglobulin-domain proteins required for maintenance of ventral nerve cord organization. *Science* **295**, 686–690.
- Ba, W., van der Raadt, J. and Nadif Kasri, N. (2013). Rho GTPase signaling at the synapse: implications for intellectual disability. *Exp. Cell Res.* **319**, 2368–2374.
- Badenhorst, P., Voas, M., Rebay, I. and Wu, C. (2002). Biological functions of the ISWI chromatin remodeling complex NURF. *Genes Dev.* **16**, 3186–3198.
- Baker, L. A., Allis, C. D. and Wang, G. G. (2008). PHD fingers in human diseases: disorders arising from misinterpreting epigenetic marks. *Mutat. Res.* **647**, 3–12.
- Barak, O., Lazzaro, M. A., Lane, W. S., Speicher, D. W., Picketts, D. J. and Shiekhattar, R. (2003). Isolation of human NURF: a regulator of Engrailed gene expression. *EMBO J.* **22**, 6089–6100.
- Barski, A., Cuddapah, S., Cui, K., Roh, T.-Y., Schones, D. E., Wang, Z., Wei, G., Chepelev, I. and Zhao, K. (2007). High-resolution profiling of histone methylations in the human genome. *Cell* **129**, 823–837.
- Bashaw, G. J., Kidd, T., Murray, D., Pawson, T. and Goodman, C. S. (2000). Repulsive axon guidance: Abelson and Enabled play opposing roles downstream of the roundabout receptor. *Cell* **101**, 703–715.
- Bear, J. E. and Gertler, F. B. (2009). Ena/VASP: towards resolving a pointed controversy at the barbed end. *J. Cell Sci.* **122**, 1947–1953.
- Beltzner, C. C. and Pollard, T. D. (2008). Pathway of actin filament branch formation by Arp2/3 complex. *J. Biol. Chem.* **283**, 7135–7144.
- Bénard, C. Y., Boyanov, A., Hall, D. H. and Hobert, O. (2006). DIG-1, a novel giant protein, non-autonomously mediates maintenance of nervous system architecture. *Development* **133**, 3329–3340.
- Bénard, C., Tjoe, N., Boulin, T., Recio, J. and Hobert, O. (2009). The small, secreted immunoglobulin protein ZIG-3 maintains axon position in *Caenorhabditis elegans*. *Genetics* **183**, 917–927.
- Bénard, C. Y., Blanchette, C., Recio, J. and Hobert, O. (2012). The secreted immunoglobulin domain proteins ZIG-5 and ZIG-8 cooperate with L1CAM/SAX-7 to maintain nervous system integrity. *PLoS Genet.* **8**, e1002819.
- Benevolenskaya, E. V. (2007). Histone H3K4 demethylases are essential in development and differentiation. *Biochem. Cell Biol.* **85**, 435–443.
- Berdasco, M. and Esteller, M. (2013). Genetic syndromes caused by mutations in epigenetic genes. *Hum. Genet.* **132**, 359–383.
- Blanchoin, L., Pollard, T. D. and Mullins, R. D. (2000). Interactions of ADF/cofilin, Arp2/3 complex, capping protein and profilin in remodeling of branched actin filament networks. *Curr. Biol.* **10**, 1273–1282.
- Boulin, T., Pocock, R. and Hobert, O. (2006). A novel Eph receptor-interacting IgSF protein provides *C. elegans* motoneurons with midline guidepost function. *Curr. Biol.* **16**, 1871–1883.
- Brenner, S. (1974). The genetics of *Caenorhabditis elegans*. *Genetics* **77**, 71–94.
- Bülow, H. E., Boulin, T. and Hobert, O. (2004). Differential functions of the *C. elegans* FGF receptor in axon outgrowth and maintenance of axon position. *Neuron* **42**, 367–374.
- Castellano, F., Montcourier, P., Guillemot, J.-C., Gouin, E., Machesky, L., Cossart, P. and Chavrier, P. (1999). Inducible recruitment of Cdc42 or WASP to a cell-surface receptor triggers actin polymerization and filopodium formation. *Curr. Biol.* **9**, 351–361.
- Catchpole, S., Spencer-Dene, B., Hall, D., Santangelo, S., Rosewell, I., Guenatri, M., Beatson, R., Scibetta, A. G., Burchell, J. M. and Taylor-Papadimitriou, J. (2011). PLU-1/JARID1B/KDM5B is required for embryonic survival and contributes to cell proliferation in the mammary gland and in ER+ breast cancer cells. *Int. J. Oncol.* **38**, 1267–1277.
- Chang, C., Adler, C. E., Krause, M., Clark, S. G., Gertler, F. B., Tessier-Lavigne, M. and Bargmann, C. I. (2006). MIG-10/lamellipodin and AGE-1/PI3K promote axon guidance and outgrowth in response to slit and netrin. *Curr. Biol.* **16**, 854–862.
- Chia, P. H., Chen, B., Li, P., Rosen, M. K. and Shen, K. (2014). Local F-actin network links synapse formation and axon branching. *Cell* **156**, 208–220.
- Christensen, J., Agger, K., Cloos, P. A. C., Pasini, D., Rose, S., Sennels, L., Rappoport, J., Hansen, K. H., Salcini, A. E. and Helin, K. (2007). RBP2 belongs to a family of demethylases, specific for tri-and dimethylated lysine 4 on histone 3. *Cell* **128**, 1063–1076.

- Cox, B. J., Vollmer, M., Tamplin, O., Lu, M., Biechele, S., Gertsenstein, M., van Campenhout, C., Floss, T., Kuhn, R., Wurst, W. et al.** (2010). Phenotypic annotation of the mouse X chromosome. *Genome Res.* **20**, 1154-1164.
- De Rubeis, S., He, X., Goldberg, A. P., Poultney, C. S., Samocha, K., Cicek, A. E., Kou, Y., Liu, L., Fromer, M., Walker, S. et al.** (2014). Synaptic, transcriptional and chromatin genes disrupted in autism. *Nature* **515**, 209-215.
- Dent, E. W., Gupton, S. L. and Gertler, F. B.** (2011). The growth cone cytoskeleton in axon outgrowth and guidance. *Cold Spring Harb. Perspect. Biol.* **3**, a001800.
- Drees, F. and Gertler, F. B.** (2008). Ena/VASP: proteins at the tip of the nervous system. *Curr. Opin. Neurobiol.* **18**, 53-59.
- Eissenberg, J. C. and Shilatifard, A.** (2010). Histone H3 lysine 4 (H3K4) methylation in development and differentiation. *Dev. Biol.* **339**, 240-249.
- Forsthöfel, D. J., Liebl, E. C., Kolodziej, P. A. and Seeger, M. A.** (2005). The Abelson tyrosine kinase, the Trio GEF and Enabled interact with the Netrin receptor Frazzled in *Drosophila*. *Development* **132**, 1983-1994.
- Fortschegger, K. and Shiekhattar, R.** (2011). Plant homeodomain fingers form a helping hand for transcription. *Epigenetics* **6**, 4-8.
- Gitai, Z., Yu, T. W., Lundquist, E. A., Tessier-Lavigne, M. and Bargmann, C. I.** (2003). The netrin receptor UNC-40/DCC stimulates axon attraction and outgrowth through enabled and, in parallel, Rac and UNC-115/AbLIM. *Neuron* **37**, 53-65.
- Gomez, T. M. and Letourneau, P. C.** (2014). Actin dynamics in growth cone motility and navigation. *J. Neurochem.* **129**, 221-234.
- Gonçalves, T. F., Gonçalves, A. P., Fintelman Rodrigues, N., dos Santos, J. M., Pimentel, M. M. G. and Santos-Reboucas, C. B.** (2014). KDM5C mutational screening among males with intellectual disability suggestive of X-Linked inheritance and review of the literature. *Eur. J. Med. Genet.* **57**, 138-144.
- Greer, E. L. and Shi, Y.** (2012). Histone methylation: a dynamic mark in health, disease and inheritance. *Nat. Rev. Genet.* **13**, 343-357.
- Greer, E. L., Maures, T. J., Hauswirth, A. G., Green, E. M., Leeman, D. S., Maro, G. S., Han, S., Banko, M. R., Gozani, O. and Brunet, A.** (2010). Members of the H3K4 trimethylation complex regulate lifespan in a germline-dependent manner in *C. elegans*. *Nature* **466**, 383-387.
- Greer, E. L., Maures, T. J., Ucar, D., Hauswirth, A. G., Mancini, E., Lim, J. P., Benayoun, B. A., Shi, Y. and Brunet, A.** (2011). Transgenerational epigenetic inheritance of longevity in *Caenorhabditis elegans*. *Nature* **479**, 365-371.
- Hatten, M. E.** (2002). New directions in neuronal migration. *Science* **297**, 1660-1663.
- Helin, K. and Dhanak, D.** (2013). Chromatin proteins and modifications as drug targets. *Nature* **502**, 480-488.
- Hobert, O. and Bülow, H.** (2003). Development and maintenance of neuronal architecture at the ventral midline of *C. elegans*. *Curr. Opin. Neurobiol.* **13**, 70-78.
- Hu, W. F., Chahrour, M. H. and Walsh, C. A.** (2014). The diverse genetic landscape of neurodevelopmental disorders. *Annu. Rev. Genomics Hum. Genet.* **15**, 195-213.
- Iossifov, I., O'Roak, B. J., Sanders, S. J., Ronemus, M., Krumm, N., Levy, D., Stessman, H. A., Witherspoon, K. T., Vives, L., Patterson, K. E. et al.** (2014). The contribution of de novo coding mutations to autism spectrum disorder. *Nature* **515**, 216-221.
- Iwase, S., Lan, F., Bayliss, P., de la Torre-Ubieta, L., Huarte, M., Qi, H. H., Whetstone, J. R., Bonni, A., Roberts, T. M. and Shi, Y.** (2007). The X-linked mental retardation gene SMCX/JARID1C defines a family of histone H3 lysine 4 demethylases. *Cell* **128**, 1077-1088.
- Kalil, K. and Dent, E. W.** (2005). Touch and go: guidance cues signal to the growth cone cytoskeleton. *Curr. Opin. Neurobiol.* **15**, 521-526.
- Kessels, M. M., Schwintzer, L., Schlobinski, D. and Qualmann, B.** (2011). Controlling actin cytoskeletal organization and dynamics during neuronal morphogenesis. *Eur. J. Cell Biol.* **90**, 926-933.
- Killeen, M. T. and Sybengco, S. S.** (2008). Netrin, Slit and Wnt receptors allow axons to choose the axis of migration. *Dev. Biol.* **323**, 143-151.
- Kleine-Kohlbrecher, D., Christensen, J., Vandamme, J., Abarrategui, I., Bak, M., Tommerup, N., Shi, X., Gozani, O., Rappaport, J., Salcini, A. E. et al.** (2010). A functional link between the histone demethylase PHF8 and the transcription factor ZNF711 in X-linked mental retardation. *Mol. Cell* **38**, 165-178.
- Klose, R. J., Yan, Q., Tothova, Z., Yamane, K., Erdjument-Bromage, H., Tempst, P., Gilliland, D. G., Zhang, Y. and Kaelin, W. G., Jr.** (2007). The retinoblastoma binding protein RBP2 is an H3K4 demethylase. *Cell* **128**, 889-900.
- Kolasinska-Zwierz, P., Down, T., Latorre, I., Liu, T., Liu, X. S. and Ahringer, J.** (2009). Differential chromatin marking of introns and expressed exons by H3K36me3. *Nat. Genet.* **41**, 376-381.
- Koleske, A. J.** (2003). Do filopodia enable the growth cone to find its way? *Sci. STKE* **2003**, pe20.
- Kooistra, S. M. and Helin, K.** (2012). Molecular mechanisms and potential functions of histone demethylases. *Nat. Rev. Mol. Cell Biol.* **13**, 297-311.
- Lazzaro, M. A. and Picketts, D. J.** (2001). Cloning and characterization of the murine Imprinting Switch (ISWI) genes: differential expression patterns suggest distinct developmental roles for Snf2h and Snf2l. *J. Neurochem.* **77**, 1145-1156.
- Lebrand, C., Dent, E. W., Strasser, G. A., Lanier, L. M., Krause, M., Svitkina, T. M., Borisy, G. G. and Gertler, F. B.** (2004). Critical role of Ena/VASP proteins for filopodia formation in neurons and in function downstream of netrin-1. *Neuron* **42**, 37-49.
- Li, H., Ilin, S., Wang, W., Duncan, E. M., Wysocka, J., Allis, C. D. and Patel, D. J.** (2006). Molecular basis for site-specific read-out of histone H3K4me3 by the BPTF PHD finger of NURF. *Nature* **442**, 91-95.
- Luo, L.** (2002). Actin cytoskeleton regulation in neuronal morphogenesis and structural plasticity. *Annu. Rev. Cell Dev. Biol.* **18**, 601-635.
- Martinez-Quiles, N., Rohatgi, R., Anton, I. M., Medina, M., Saville, S. P., Miki, H., Yamaguchi, H., Takenawa, T., Hartwig, J. H., Geha, R. S. et al.** (2001). WIP regulates N-WASP-mediated actin polymerization and filopodium formation. *Nat. Cell Biol.* **3**, 484-491.
- Matthews, A. G. W., Kuo, A. J., Ramon-Maiques, S., Han, S., Champagne, K. S., Ivanov, D., Gallardo, M., Carney, D., Cheung, P., Ciccone, D. N. et al.** (2007). RAG2 PHD finger couples histone H3 lysine 4 trimethylation with V(D)J recombination. *Nature* **450**, 1106-1110.
- Mello, C. C., Kramer, J. M., Stinchcombe, D. and Ambros, V.** (1991). Efficient gene transfer in *C. elegans*: extrachromosomal maintenance and integration of transforming sequences. *EMBO J.* **10**, 3959-3970.
- Miki, H., Sasaki, T., Takai, Y. and Takenawa, T.** (1998). Induction of filopodium formation by a WASP-related actin-depolymerizing protein N-WASP. *Nature* **391**, 93-96.
- Mizuguchi, G., Tsukiyama, T., Wisniewski, J. and Wu, C.** (1997). Role of nucleosome remodeling factor NURF in transcriptional activation of chromatin. *Mol. Cell* **1**, 141-150.
- Mohamed, A. M., Boudreau, J. R., Yu, F. P. S., Liu, J. and Chin-Sang, I. D.** (2012). The *Caenorhabditis elegans* Eph receptor activates NCK and N-WASP, and inhibits Ena/VASP to regulate growth cone dynamics during axon guidance. *PLoS Genet.* **8**, e1002513.
- Musselman, C. A. and Kutateladze, T. G.** (2011). Handpicking epigenetic marks with PHD fingers. *Nucleic Acids Res.* **39**, 9061-9071.
- Nadif Kasri, N. and Van Aelst, L.** (2008). Rho-linked genes and neurological disorders. *Pflugers Arch.* **455**, 787-797.
- Najmabadi, H., Hu, H., Garshasbi, M., Zemojtel, T., Abedini, S. S., Chen, W., Hosseini, M., Behjati, F., Haas, S., Jamali, P. et al.** (2011). Deep sequencing reveals 50 novel genes for recessive cognitive disorders. *Nature* **478**, 57-63.
- Norris, A. D., Dyer, J. O. and Lundquist, E. A.** (2009). The Arp2/3 complex, UNC-115/AbLIM, and UNC-34/Enabled regulate axon guidance and growth cone filopodia formation in *Caenorhabditis elegans*. *Neural Dev.* **4**, 38.
- Palacios, A., Muñoz, I. G., Pantoja-Uceda, D., Marcaida, M. J., Torres, D., Martín-García, J. M., Luque, I., Montoya, G. and Blanco, F. J.** (2008). Molecular basis of histone H3K4me3 recognition by ING4. *J. Biol. Chem.* **283**, 15956-15964.
- Pantalon, D., Boujemaa, R., Didry, D., Gounon, P. and Carlier, M.-F.** (2000). The Arp2/3 complex branches filament barbed ends: functional antagonism with capping proteins. *Nat. Cell Biol.* **2**, 385-391.
- Pedersen, M. T. and Helin, K.** (2010). Histone demethylases in development and disease. *Trends Cell Biol.* **20**, 662-671.
- Peña, P. V., Davrazou, F., Shi, X., Walter, K. L., Verkhusha, V. V., Gozani, O., Zhao, R. and Kutateladze, T. G.** (2006). Molecular mechanism of histone H3K4me3 recognition by plant homeodomain of ING2. *Nature* **442**, 100-103.
- Pocock, R., Bénard, C. Y., Shapiro, L. and Hobert, O.** (2008). Functional dissection of the *C. elegans* cell adhesion molecule SAX-7, a homologue of human L1. *Mol. Cell. Neurosci.* **37**, 56-68.
- Pollitt, A. Y. and Insall, R. H.** (2009). WASP and SCAR/WAVE proteins: the drivers of actin assembly. *J. Cell Sci.* **122**, 2575-2578.
- Rivero-Lezcano, O. M., Marcilla, A., Sameshima, J. H. and Robbins, K. C.** (1995). Wiskott-Aldrich syndrome protein physically associates with Nck through Src homology 3 domains. *Mol. Cell. Biol.* **15**, 5725-5731.
- Rohatgi, R., Nollau, P., Ho, H.-Y. H., Kirschner, M. W. and Mayer, B. J.** (2001). Nck and phosphatidylinositol 4,5-bisphosphate synergistically activate actin polymerization through the N-WASP-Arp2/3 pathway. *J. Biol. Chem.* **276**, 26448-26452.
- Ronan, J. L., Wu, W. and Crabtree, G. R.** (2013). From neural development to cognition: unexpected roles for chromatin. *Nat. Rev. Genet.* **14**, 347-359.
- Sawa, M. and Takenawa, T.** (2006). *Caenorhabditis elegans* WASP-interacting protein homologue WIP-1 is involved in morphogenesis through maintenance of WSP-1 protein levels. *Biochem. Biophys. Res. Commun.* **340**, 709-717.
- Schmitz, S. U., Albert, M., Malatesta, M., Morey, L., Johansen, J. V., Bak, M., Tommerup, N., Abarrategui, I. and Helin, K.** (2011). Jarid1b targets genes regulating development and is involved in neural differentiation. *EMBO J.* **30**, 4586-4600.
- Shakir, M. A., Jiang, K., Struckhoff, E. C., Demarco, R. S., Patel, F. B., Soto, M. C. and Lundquist, E. A.** (2008). The Arp2/3 activators WAVE and WASP have distinct genetic interactions with Rac GTPases in *Caenorhabditis elegans* axon guidance. *Genetics* **179**, 1957-1971.
- Shekarabi, M., Moore, S. W., Tritsch, N. X., Morris, S. J., Bouchard, J.-F. and Kennedy, T. E.** (2005). Deleted in colorectal cancer binding netrin-1 mediates cell substrate adhesion and recruits Cdc42, Rac1, Pak1, and N-WASP into an intracellular signaling complex that promotes growth cone expansion. *J. Neurosci.* **25**, 3132-3141.

- Shen, E., Shulha, H., Weng, Z. and Akbarian, S.** (2014). Regulation of histone H3K4 methylation in brain development and disease. *Philos. Trans. R. Soc. Lond. B Biol. Sci.* **369**, 20130514.
- Shi, X., Hong, T., Walter, K. L., Ewalt, M., Michishita, E., Hung, T., Carney, D., Peña, P., Lan, F., Kaadige, M. R. et al.** (2006). ING2 PHD domain links histone H3 lysine 4 methylation to active gene repression. *Nature* **442**, 96-99.
- Sims, R. J., III and Reinberg, D.** (2006). Histone H3 Lys 4 methylation: caught in a bind? *Genes Dev.* **20**, 2779-2786.
- Srivastava, A. K. and Schwartz, C. E.** (2014). Intellectual disability and autism spectrum disorders: causal genes and molecular mechanisms. *Neurosci. Biobehav. Rev.* **46**, 161-174.
- Sulston, J. E., Schierenberg, E., White, J. G. and Thomson, J. N.** (1983). The embryonic cell lineage of the nematode *Caenorhabditis elegans*. *Dev. Biol.* **100**, 64-119.
- Suzuki, H., Maruyama, R., Yamamoto, E. and Kai, M.** (2013). Epigenetic alteration and microRNA dysregulation in cancer. *Front. Genet.* **4**, 258.
- Symons, M., Derry, J. M. J., Karlak, B., Jiang, S., Lemahieu, V., McCormick, F., Francke, U. and Abo, A.** (1996). Wiskott-Aldrich syndrome protein, a novel effector for the GTPase CDC42Hs, is implicated in actin polymerization. *Cell* **84**, 723-734.
- Tahirovic, S., Hellal, F., Neukirchen, D., Hindges, R., Garvalov, B. K., Flynn, K. C., Stradal, T. E., Chrostek-Grashoff, A., Brakebusch, C. and Bradke, F.** (2010). Rac1 regulates neuronal polarization through the WAVE complex. *J. Neurosci.* **30**, 6930-6943.
- Takenawa, T. and Suetsugu, S.** (2007). The WASP-WAVE protein network: connecting the membrane to the cytoskeleton. *Nat. Rev. Mol. Cell Biol.* **8**, 37-48.
- Vallianatos, C. N. and Iwase, S.** (2015). Disrupted intricacy of histone H3K4 methylation in neurodevelopmental disorders. *Epigenomics* **7**, 503-519.
- Vermeulen, M. and Timmers, H. T. M.** (2010). Grasping trimethylation of histone H3 at lysine 4. *Epigenomics* **2**, 395-406.
- Vermeulen, M., Mulder, K. W., Denissov, S., Pijnappel, W. W. M. P., van Schaik, F. M. A., Varier, R. A., Baltissen, M. P. A., Stunnenberg, H. G., Mann, M. and Timmers, H. T. M.** (2007). Selective anchoring of TFIID to nucleosomes by trimethylation of histone H3 lysine 4. *Cell* **131**, 58-69.
- White, J. G., Southgate, E., Thomson, J. N. and Brenner, S.** (1986). The structure of the nervous system of the nematode *Caenorhabditis elegans*. *Philos. Trans. R. Soc. Lond. B Biol. Sci.* **314**, 1-340.
- Woo, W.-M., Berry, E. C., Hudson, M. L., Swale, R. E., Goncharov, A. and Chisholm, A. D.** (2008). The *C. elegans* F-spondin family protein SPON-1 maintains cell adhesion in neural and non-neuronal tissues. *Development* **135**, 2747-2756.
- Wysocka, J., Swigut, T., Xiao, H., Milne, T. A., Kwon, S. Y., Landry, J., Kauer, M., Tackett, A. J., Chait, B. T., Badenhorst, P. et al.** (2006). A PHD finger of NURF couples histone H3 lysine 4 trimethylation with chromatin remodelling. *Nature* **442**, 86-90.
- Yamaguchi, H., Miki, H., Suetsugu, S., Ma, L., Kirschner, M. W. and Takenawa, T.** (2000). Two tandem verprolin homology domains are necessary for a strong activation of Arp2/3 complex-induced actin polymerization and induction of microspike formation by N-WASP. *Proc. Natl. Acad. Sci. USA* **97**, 12631-12636.
- Yu, T. W., Hao, J. C., Lim, W., Tessier-Lavigne, M. and Bargmann, C. I.** (2002). Shared receptors in axon guidance: SAX-3/Robo signals via UNC-34/Enabled and a Netrin-independent UNC-40/DCC function. *Nat. Neurosci.* **5**, 1147-1154.
- Zallen, J. A., Cohen, Y., Hudson, A. M., Cooley, L., Wieschaus, E. and Schejter, E. D.** (2002). SCAR is a primary regulator of Arp2/3-dependent morphological events in *Drosophila*. *J. Cell Biol.* **156**, 689-701.
- Zhang, G. and Pradhan, S.** (2014). Mammalian epigenetic mechanisms. *IUBMB Life* **66**, 240-256.
- Zhang, Y., Chen, D., Smith, M. A., Zhang, B. and Pan, X.** (2012). Selection of reliable reference genes in *Caenorhabditis elegans* for analysis of nanotoxicity. *PLoS ONE* **7**, e31849.

## SUPPLEMENTARY INFORMATION

**A****B**

**Fig. S1.** (A) Left: Representative images of HSN neurons in wild-type (WT) and *rbr-2(tm3141)* adult animals, visualized using the transgene *rpEx6*. Ventral views, anterior to the left. Scale bar, 20  $\mu$ m. Asterisk indicates aberrant position of the cell body. Center: Schematic diagrams of HSN neurons in wild-type and *rbr-2(tm3141)* mutant animals. Right: Quantification of HSN aberrant cell migration in *rbr-2(tm3141)* adult animals.  $n>100$ , \*p<0.05 (Fisher's exact test). Error bars represent standard error of proportion. (B) Left: Quantification of PVQ axonal cross-over defects in *rbr-2(tm1231)* mutant animals.  $n=100$ , \*\*\*\*p<0.0001 (Fisher's exact test). Error bars represent standard error of proportion. Right, top: Genomic organization of *rbr-2*. Black H-shaped line indicates the position of the *tm1231* deletion. Right, bottom: RBR-2 and putative *tm1231* protein. JmjN, Jumonji N domain; ARID, AT-rich interacting domain; PHD, plant homeodomain zinc-finger domain; JmjC, Jumonji C domain; Zf, zinc-finger.

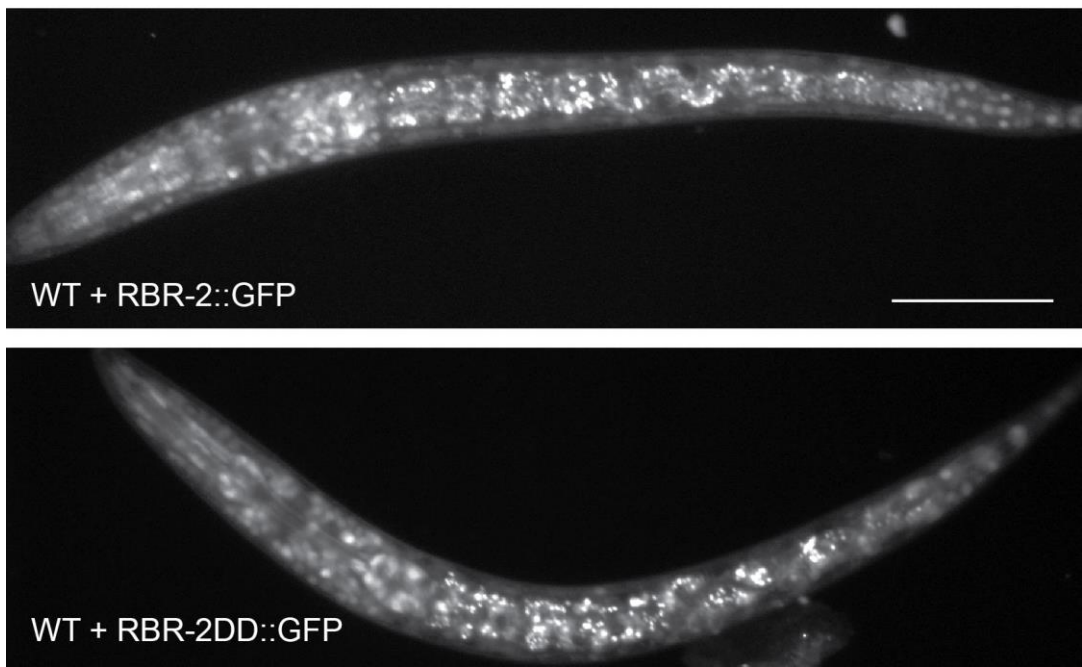


**Fig. S2.** Representative images of wild-type (WT) L1 animals expressing GFP-tagged RBR-2 or catalytically inactive RBR-2 (RBR-2DD). Ventral view, anterior to the left. Scale bar, 35  $\mu$ m.

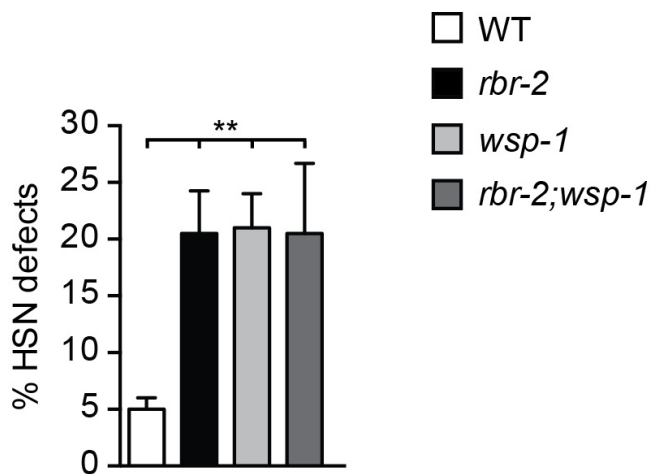


**Fig. S3.** Quantification of HSN axonal cross-over defects in *rbr-2(tm3141)*, *wsp-1(gm324)* and double mutant.  $n>100$ , \*\* $p<0.01$  (one-way ANOVA followed by Tukey's multiple-comparison test). Error bars represent standard error of proportion.

**Table S1.** *rbr-2* genetically interacts with the main pathways involved in axon guidance

Genotype	Defective animals (%)
WT	9 (n=162)
<i>rbr-2(tm3141)</i>	22 (n=296)
<i>unc-5(e53)</i>	25 (n=200)
<i>rbr-2(tm3141);unc-5(e53)</i>	33 (n=200) n.s.
<i>sax-3(ky123)</i>	52 (n=96)
<i>rbr-2(tm3141);sax-3(ky123)</i>	45 (n=112) n.s.
<i>slt-1(eh15)</i>	23 (n=150)
<i>rbr-2(tm3141);slt-1(eh15)</i>	27 (n=150) n.s.
<i>vab-1(dx31)</i>	27 (n=210)
<i>rbr-2(tm3141);vab-1(dx31)</i>	26 (n=218) n.s.
<i>vab-2(ju1)</i>	15 (n=100)
<i>rbr-2(tm3141);vab-2(ju1)</i>	19 (n=200) n.s.
<i>efn-3(ev696)</i>	34 (n=50)
<i>rbr-2(tm3141);efn-3(ev696)</i>	34 (n=200) n.s.
<i>vab-2(ju1);efn-3(ev696)</i>	32 (n=100)
<i>rbr-2(tm3141);vab-2(ju1);efn-3(ev696)</i>	39 (n=200) n.s.
<i>hse-5(tm472)</i>	45 (n=150)
<i>rbr-2(tm3141);hse-5(tm472)</i>	40 (n=150) n.s.
<i>sdn-1(zh20)</i>	47 (n=150)
<i>rbr-2(tm3141);sdn-1(zh20)</i>	42 (n=150) n.s.
<i>plx-2(ev773)</i>	27 (n=200)
<i>rbr-2(tm3141);plx-2(ev773)</i>	20 (n=200) n.s.

Quantification of PVQ axonal cross-over defects in the indicated strains. Statistical significance of the difference between double mutants and the corresponding single mutant with the highest penetrance was assessed with one-way ANOVA followed by Tukey's multiple-comparison test. n.s., not significant.

**Table S2. Mammalian PHD-containing proteins binding to H3K4me3 and their *C. elegans* homologs**

Mammalian protein	<i>C. elegans</i> homolog	Allele
BPTF	NURF-1	<i>nurf-1(n4295)</i>
ING1/5	LSY-13 ING-3 Y43H11AL.1	<i>lsy-13(ok1475)</i> <i>ing-3(tm2530)</i> not available
KDM7A/C	JMJD-1.1 JMJD-1.2	<i>jmjd-1.1(tm3980)</i> <i>jmjd-1.2(tm3713)</i>
RAG2	-	-
TAF3	TAF-3	not available

List of plant homeodomain (PHD)-containing proteins reported to bind H3K4me3 in mammals (Fortschegger and Shiekhattar, 2011), homologs in *C. elegans* and mutant alleles used in this study.

**Table S3. Loss of *nurf-1* restores correct PVQ guidance in *rbr-2(tm3141)* mutants**

<b>Genotype</b>	<b>Defective animals (%)</b>
WT	9 (n=162)
<i>rbr-2(tm3141)</i>	22 (n=296)
<i>nurf-1(n4295)</i>	14 (n=150)
<i>rbr-2(tm3141);nurf-1(n4295)</i>	12 (n=150) **
<i>ing-3(tm2530)</i>	14 (n=100)
<i>rbr-2(tm3141);ing-3(tm2530)</i>	23 (n=100) n.s.
<i>lsy-13(ok1475)</i>	9 (n=100)
<i>rbr-2(tm3141);lsy-13(ok1475)</i>	17 (n=150) n.s.
<i>jmjd-1.1(tm3980)</i>	n.d.
<i>rbr-2(tm3141);jmjd-1.1(tm3980)</i>	26 (n=100) n.s.
<i>jmjd-1.2(tm3713)</i>	22 (n=200)
<i>rbr-2(tm3141);jmjd-1.2(tm3713)</i>	17 (n=200) n.s.

Quantification of PVQ axonal cross-over defects in the indicated strains. Statistical significance of the difference between *rbr-2(tm3141)* and double mutants was assessed with one-way ANOVA followed by Tukey's multiple-comparison test. \*\*p<0.01, n.s., not significant, n.d., not determined. For unclear reasons, it was not possible to obtain the single mutant *jmjd-1.1(tm3980)* carrying a transgenic marker for the PVQs.

**Table S4. Transgenic strains**

Strain	Genotype
ZR241	N2; <i>zrEx48 Ex(Prbr-2::rbr-2::GFP)</i>
ZR246	<i>rbr-2(tm3141); oyIs14; zrEx48 Ex(Prbr-2::rbr-2::GFP)</i>
ZR848	<i>rbr-2(tm3141); oyIs14; zrEx289 Ex(Prbr-2::rbr-2::GFP)</i>
ZR849	<i>rbr-2(tm3141); oyIs14; zrEx290 Ex(Prbr-2::rbr-2::GFP)</i>
ZR248	<i>rbr-2(tm3141); oyIs14; zrEx51 Ex(PF25B3.3::rbr-2::GFP)</i>
ZR412	<i>rbr-2(tm3141); oyIs14; zrEx87 Ex(PF25B3.3::rbr-2::GFP)</i>
ZR413	<i>rbr-2(tm3141); oyIs14; zrEx88 Ex(PF25B3.3::rbr-2::GFP)</i>
ZR249	<i>rbr-2(tm3141); oyIs14; zrEx50 Ex(Pmyo-3::rbr-2::GFP)</i>
ZR408	<i>rbr-2(tm3141); hdIs26; zrEx83 Ex(Pmyo-3::rbr-2::GFP)</i>
ZR409	<i>rbr-2(tm3141); hdIs26; zrEx84 Ex(Pmyo-3::rbr-2::GFP)</i>
ZR851	<i>rbr-2(tm3141); oyIs14; zrEx291 Ex(Pdpy-7::rbr-2::GFP)</i>
ZR852	<i>rbr-2(tm3141); oyIs14; zrEx292 Ex(Pdpy-7::rbr-2::GFP)</i>
ZR594	<i>rbr-2(tm3141); oyIs14; zrEx175 Ex(Psra-6::rbr-2::GFP)</i>
ZR595	<i>rbr-2(tm3141); oyIs14; zrEx176 Ex(Psra-6::rbr-2::GFP)</i>
ZR597	<i>rbr-2(tm3141); oyIs14; zrEx178 Ex(Psra-6::rbr-2::GFP)</i>
ZR242	N2; <i>zrEx49 Ex(Prbr-2::rbr-2DD::GFP)</i>
ZR247	<i>rbr-2(tm3141); oyIs14; zrEx49 Ex(Prbr-2::rbr-2DD::GFP)</i>
ZR293	<i>rbr-2(tm3141); hdIs26; zrEx66 Ex(Prbr-2::rbr-2DD::GFP)</i>
ZR294	<i>rbr-2(tm3141); hdIs26; zrEx67 Ex(Prbr-2::rbr-2DD::GFP)</i>
ZR850	N2; <i>Is(Prbr-2::rbr-2::GFP)</i>
ZR677	N2; <i>oyIs14; zrEx217 Ex(PF25B3.3::wsp-1a cDNA)</i>
ZR679	N2; <i>oyIs14; zrEx219 Ex(PF25B3.3::wsp-1a cDNA)</i>

Strain	Genotype
ZR680	N2; <i>oyIs14</i> ; <i>zrEx220</i> Ex( <i>PF25B3.3::wsp-1a</i> cDNA)
ZR839	N2; <i>oyIs14</i> ; <i>zrEx280</i> Ex( <i>Pmyo-3::wsp-1a</i> cDNA)
ZR840	N2; <i>oyIs14</i> ; <i>zrEx281</i> Ex( <i>Pmyo-3::wsp-1a</i> cDNA)
ZR842	N2; <i>oyIs14</i> ; <i>zrEx283</i> Ex( <i>Pmyo-3::wsp-1a</i> cDNA)
ZR846	<i>rbr-2(tm3141);wsp-1(gm324); oyIs14; zrEx217</i> Ex( <i>PF25B3.3::wsp-1a</i> cDNA)
ZR847	<i>rbr-2(tm3141);wsp-1(gm324); oyIs14; zrEx288</i> Ex( <i>PF25B3.3::wsp-1a</i> cDNA::GFP)
ZR900	N2; <i>oyIs14</i> ; <i>zrEx321</i> Ex( <i>PF25B3.3::VCA</i> cDNA::GFP)
ZR901	N2; <i>oyIs14</i> ; <i>zrEx322</i> Ex( <i>PF25B3.3::VCA</i> cDNA::GFP)
ZR902	N2; <i>oyIs14</i> ; <i>zrEx323</i> Ex( <i>PF25B3.3::VCA</i> cDNA::GFP)
ZR905	N2; <i>oyIs14</i> ; <i>zrEx326</i> Ex( <i>Psra-6::VCA</i> cDNA::GFP)
ZR906	N2; <i>oyIs14</i> ; <i>zrEx327</i> Ex( <i>Psra-6::VCA</i> cDNA::GFP)
ZR910	N2; <i>oyIs14</i> ; <i>zrEx331</i> Ex( <i>Psra-6::VCA</i> cDNA::GFP)]

List of transgenic strains used in this study: names and genotypes are indicated.